THE UNIVERSITY OF OKLAHOMA

GRADUATE COLLEGE

QUADRATURE VARIATIONS IN DISCRETE ORDINATES CALCULATIONS

A DISSERTATION

SUBMITTED TO THE GRADUATE FACULTY

in partial fulfillment of the requirements for the

degree of

DOCTOR OF PHILOSOPHY

BY

ROBERT EMMETT SULLIVAN

Norman, Oklahoma

1971

QUADRATURE VARIATIONS IN DISCRETE

ORDINATES CALCULATIONS

APPROVED BY

Baksoon Yu

Lynn D. Albers

J. E. Frances

W. A. Rhoades

M. L. Rasmussen

DISSERTATION COMMITTEE

ACKNOWLEDGEMENT

The author wishes to express his sincere gratitude to the many individuals from whom assistance and encouragement in the preparation of this dissertation have been obtained. Particular appreciation is due Dr. Dahsoong Yu, the dissertation committee chairman, for his continuing advice and suggestions concerning the work undertaken. The author also wishes to thank the committee co-chairman, Dr. Lynn U. Albers, for his interest and assistance.

The author also gratefully acknowledges the financial and other assistance provided by the National Aeronautics and Space Administration.

TABLE OF CONTENTS

	Page
LIST OF TABLES	v
LIST OF ILLUSTRATIONS	vi
Chapter	
I. INTRODUCTION	1
II. REVIEW OF PREVIOUS WORK	9
III. THE DISCRETE ORDINATES (S_n) METHOD	15
IV. QUADRATURE VARIATIONS	29
V. VERIFICATION OF NUMERICAL METHODS	99
VI. DISCUSSION OF RESULTS AND CONCLUSIONS	110
LIST OF REFERENCES	117
APPENDIX - NOMENCLATURE	122

LIST OF TABLES

Table		Page
1.	Scalar Flux Distribution in Standard and Fully Decoupled S_6 Quadratures	54
2.	Scalar Flux Distribution in ($\sigma^a = \sigma^s = 0.5$) Test Case	60
3.	Scalar Flux Distribution in ($\sigma^a = \sigma^s = 0.5$) Decoupled Higher Orders	61
4.	Scalar Flux Distribution in ($\sigma^s = \sigma^a = 0.05$) Test Case	65
5.	Energy Groups and Cross-Sections for Quadrature Variation Problems	79
6.	Angular Quadrature Variations (S_8 Final)	85
7.	Angular Quadrature Variations (S_{16} Final)	86
8.	Calculation of Exact Critical Radii	108

LIST OF ILLUSTRATIONS

Figure		Page
1.	Rectangular Coordinate System Spatial Mesh Cell	17
2.	Unit Direction Vector Coordinates	18
3.	Spatial-Angular Quadrature Flow Diagram	26
4.	Incorrect Angular Flux Averaging	46
5.	Ray Effect Sample Geometry	53
6.	Decoupling of Standard S_6 Quadrature Set	56
7.	Independent S_4 Sets to Replace Standard S_6 Set . .	58
8.	Scalar Flux Distribution in S_6 Quadrature Variations	59
9.	Decoupling of Standard S_8 Quadrature Set	62
10.	Decoupling of Standard S_{12} Quadrature Set	63
11.	Scalar Flux Comparisons in Reduced Scattering Test Case	66
12.	Scalar Flux Comparisons in Fission Source Test Case . .	68
13.	Spatial and Material Base Case Test Configuration . . .	78
14.	Spatial Mesh Interval Truncation Variation	92
15.	Spatial Mesh Combination Example	95
16.	Spatial Mesh Interval Combination Variation	96
17.	Approach to Exact Eigenvalue through Ascending Quadrature Orders	109

QUADRATURE VARIATIONS IN THE DISCRETE ORDINATES APPROXIMATION TO THE BOLTZMANN TRANSPORT EQUATION

CHAPTER I

INTRODUCTION

The fundamental problem in nuclear reactor theory is the determination of the neutron distribution $N(\vec{r}, E, \hat{\Omega}, t)$ as a function of space, energy, direction, and time. The migration of such particles through various media is most accurately described by the Boltzmann transport equation [1]. In its most general form, the transport equation describes the behaviour of an inhomogeneous mixture of mutually interacting particles. Since the neutron is an elementary, uncharged particle, several simplifying assumptions may be made when the equation is applied to nuclear reactors. These are:

(1) That neutron-neutron collisions may be neglected. This assumption is valid since, even in an extremely powerful reactor, the neutron density is negligible compared to the density of the nuclei constituting the medium.

(2) That between collisions the neutrons travel in straight lines at a constant energy. This assumption is true since the only forces of importance acting on the neutrons are short range nuclear ones.

(3) That interactions, or collisions, between the neutrons and the medium are well defined events and that neutrons emerge from a collision at the same point in space at which the collision occurred. This assumption is justifed by the nature of the nuclear forces and the relative nuclear transparency of the medium.

While the second and third assumptions would be violated if the transport equation were applied to charged particles, none of the assumptions is contradicted when photons are treated. The form of the transport equation to be used is, then, equally valid for problems involving radiative transfer in stellar atmospheres and the attenuation and scattering of X and γ rays.

The quantity of basic interest in nuclear reactors is the neutron angular flux $\psi(\vec{r}, E, \hat{\Omega}, t)$ which is defined as the product of the neutron speed, v, and density, $n(\vec{r}, E, \hat{\Omega}, t)$. In this equation,

$\vec{r}$ = the space coordinates.

E = the neutron energy in the laboratory system.

$\hat{\Omega}$ = the unit vector in the neutron direction of motion.

t = the time.

The scalar, or non-angular dependent, neutron flux is related to the angular flux by

$$\phi(\vec{r}, E, t) = \int_{\hat{\Omega}} \psi(\vec{r}, E, \hat{\Omega}, t) d\hat{\Omega} \qquad (1)$$

If the probability, per unit path length, that a neutron interact with the nuclei of the medium is defined as

$$\sigma^{x}(\vec{r}, E)$$

then one important aspect of the scalar neutron flux is immediately apparent. It is that the simple product

$$R_x(\vec{r}, E, t) = \phi(\vec{r}, E, t)\sigma^x(\vec{r}, E)$$

gives the reaction rate, $R_x(\vec{r},E,t)$, for process x.

It is now possible, using the definition for the angular flux and the assumptions previously stated, to obtain a mathematical expression for the time rate of change of the neutron density, $n(\vec{r}, E, \hat{\Omega}, t)$. Since

$$vn(r, E, \hat{\Omega}, t) = \psi(\vec{r}, E, \hat{\Omega}, t)$$

then

$$\frac{\partial n(\vec{r}, E, \hat{\Omega}, t)}{\partial t} = \frac{1}{v}\frac{\partial \psi(\vec{r}, E, \hat{\Omega}, t)}{\partial t}$$

which must be equal to the sum of all the factors contributing to the density change.

There are two basic reasons for a change in the neutron density. The position coordinates may change due to motion of the neutron or the energy-direction variables may be altered due to collision with the medium. In the absence of an interaction, due to transport of the neutrons:

$$-\Omega_x \frac{\partial \psi}{\partial x} - \Omega_y \frac{\partial \psi}{\partial y} - \Omega_z \frac{\partial \psi}{\partial z} = -\hat{\Omega} \cdot \nabla\psi$$

If an interaction with the medium occurs, the collision process may result in the neutron being scattered, σ^s, out of the energy range and direction of interest:

$$-\int dE\, d\hat{\Omega}\ \ \psi(\vec{r}, E, \hat{\Omega}, t)\left[\sigma^s(\vec{r}, E \to E', \hat{\Omega} \to \hat{\Omega}')\right]$$

If the collision results in the neutron being absorbed, σ^a,

$$-\psi(\vec{r}, E, \hat{\Omega}, t)\sigma^a(\vec{r}, E)$$

The collision may also result in a neutron being scattered into the energy-direction range of interest:

$$+\int dE'd\hat{\Omega}'\ \psi(\vec{r}, E', \hat{\Omega}', t)\ \sigma^s(\vec{r}, E' \to E, \hat{\Omega}' \to \hat{\Omega})$$

In addition, there may be other sources of neutrons such as the fission process, σ^f, neutron producing materials, or particle accelerators. For the present, let these be represented by

$$S(\vec{r}, E, \hat{\Omega}, t)$$

Summing all these terms, noting that

$$\int dE\ d\hat{\Omega}\ \ \sigma^s(r, E \to E', \hat{\Omega} \to \hat{\Omega}') = \sigma^s(r, E)$$

and defining the total cross-section, σ^t, as

$$\sigma^t(\vec{r}, E) = \sigma^a(\vec{r}, E) + \sigma^s(\vec{r}, E)$$

yields the transport equation

$$\frac{1}{v}\frac{\partial\psi(\vec{r}, E, \hat{\Omega}, t)}{\partial t} = -\hat{\Omega}\cdot\nabla\psi(\vec{r}, E, \hat{\Omega}, t) + S(\vec{r}, E, \hat{\Omega}, t)$$

$$-\psi(\vec{r}, E, \hat{\Omega}, t)\left[\sigma^t(\vec{r}, E)\right]$$

$$+\int dE'd\hat{\Omega}'\ \psi(\vec{r}, E', \hat{\Omega}', t)\left[\sigma^s(\vec{r}, E' \to E, \hat{\Omega}' \to \hat{\Omega})\right] \qquad (2)$$

which is essentially a statement of the law of conservation applied to neutrons.

The single most important application of the transport equation is the determination of the neutron flux distribution in the stationary case. Removing the time dependence from equation (2) and setting the left hand term equal to zero results in

$$\hat{\Omega} \cdot \nabla\psi(\bar{r}, E, \hat{\Omega}) + \psi(\bar{r}, E, \hat{\Omega})\, \sigma^{t}(\bar{r}, E)$$

$$= \int dE' d\hat{\Omega}'\ \psi(\bar{r}, E', \Omega')\sigma^{s}(\bar{r}, E' \rightarrow E, \hat{\Omega}' \rightarrow \Omega)$$

$$+ S(r, E, \hat{\Omega}) \qquad (3)$$

the stationary transport equation. There are two classes of problem which are of primary interest. Although the $S(\bar{r}, E, \hat{\Omega}, t)$ term was defined to include neutrons produced by the fission process, any such interaction process depends on the neutron flux and the fission production term may be combined with the total cross-section term. The remaining terms in $S(\bar{r}, E, \hat{\Omega}, t)$ are then extraneous sources in the sense that they represent neutrons introduced into the system. Under these conditions, solutions to the transport equation are seen to fall into two categories:

(1) If the extraneous source term is not zero, the problem consists of determining the resulting flux distribution in a given configuration. The equation is non-homogeneous.

(2) If the extraneous source term is zero, the problem is that of determining the nuclear or geometrical configuration for which a stationary flux distribution is possible. This equation is homogeneous.

The solutions to problems of this type constitute the main body of nuclear reactor theory. In particular, the solution to the

homogeneous equation leads to an eigenvalue problem allowing calculation of the critical size or critical mass of a reactor. The solution to the stationary equation is also of basic importance since, in theory, the time dependent problem may always be reduced to a stationary one [2]. If the Laplace transform of a function, F(t), is defined as

$$\overline{F}(s) = \int_0^\infty e^{-st} F(t)dt$$

then introducing the boundary condition that $\psi(\overline{r}, E, \hat{\Omega}, 0) = 0$ and taking the transform of equation (2) gives .

$$\frac{s}{v}\overline{\psi} = -\hat{\Omega} \cdot \nabla\psi + \overline{S} - \overline{\psi}\sigma^t + \int dE'd\hat{\Omega}'\overline{\psi}'\sigma^{s'} \qquad (4)$$

which is of the same form as equation (3) since the s/v modifying $\overline{\psi}$ in the left hand term may be combined with the right hand side to modify the definition of the total cross-section. Solutions to the stationary problem of equation (3) are then also solutions to the transformed equation (4). In practice, considerable difficulty may be encountered in finding the inverse transform. However, if the stationary equation is soluble, there are several practical methods for extending the solution to the time dependent case.

There are several physical aspects of nuclear reactor design which may be applied in considering possible solutions to equations (3) and (4) especially in the homogeneous form [3]. First, the angular flux must everywhere be finite and non-negative since negative fluxes or densities do not admit of a valid physical interpretation. Since only

one eigenfunction resulting from the solution of the homogeneous equation can meet this requirement, only the associated eigenvalue is of interest. Second, the nuclear reactor must have definite boundaries. Since the solution to an eigenvalue problem for a finite system must yield a discrete set of eigenvalues, these may be arranged in descending order. If the eigenvalues are λ_n, with λ_o the largest, then the general solution for the transformed angular flux of equation (1) may be shown to be [2]

$$\psi(\vec{r}, E, \hat{\Omega}, t) = \sum_{n=0}^{\infty} a_n \psi_{t,n}(\vec{r}, E, \hat{\Omega})\, e^{\lambda_n t}$$

so that, at large t, when the largest eigenvalue predominates

$$\psi(\vec{r}, E, \hat{\Omega}, t) \simeq a_o N_{t,o}(\vec{r}, E, \hat{\Omega})\, e^{\lambda_o t}$$

and indicates that the flux distribution changes exponentially when the reactor is perturbed. This equation is also of interest since it shows that the value of λ_o controls the behaviour of the reactor. If λ_o is negative, the system is subcritical and the flux distribution is controlled by the extraneous sources. If λ_o is exactly zero, the system is critical and the flux, and power level, remain constant. If λ_o is greater than zero, the system is supercritical and the flux and power level increase exponentially.

An additional consequence of the eigenvalue problem posed by the homogeneous transport equation is that the positive eigenfunction is determined only to within an arbitrary multiplicative constant. This indicates, as is also experimentally observable, that a change in flux

distribution caused by a variation in λ_o, which is then returned to its original value, changes only the magnitude, not the shape, of the distribution. Therefore, the neutron flux distribution found by solving the stationary transport equation is a general solution in the sense that it yields the correct distribution for a given critical reactor operating at any constant power level.

As a result of the foregoing discussion, the balance of this study will be devoted to methods for obtaining solutions to the stationary transport equation.

CHAPTER II

REVIEW OF PREVIOUS WORK

The search for methods which might be suitable for obtaining solutions to problems involving the stationary Boltzmann transport equation

$$\hat{\Omega} \cdot \nabla\psi + \psi\sigma^{t} = \int dE' d\hat{\Omega}' \psi' \sigma^{s}(\vec{r},\ E' \rightarrow E,\ \hat{\Omega}' \rightarrow \hat{\Omega}) + S \qquad (3)$$

has occupied a prominent place in the literature since the initial derivation of the equation. Much of the early literature was devoted to problems not connected with neutrons and, indeed, antedates the discovery of the neutron by many years. Some of the more important early applications of the equation were to radiation transfer and equilibrium in stellar atmospheres, penetration of photons in various media, and the study of cosmic rays. Most of this early work is characterized by the extreme nature of the assumptions made to simplify the transport equation. The type of problem considered was also less complex than that encountered in neutron reactor theory. A star, for example, is an extremely large body which is relatively homogeneous.

The assumption most widely used to simplify the transport equation is the removal of the energy dependence of equation (3). The resulting equation

$$\hat{\Omega} \cdot \nabla\psi(\vec{r},\ \hat{\Omega}) + \psi(\vec{r},\ \hat{\Omega})\sigma^{t}(\vec{r}) = \int d\hat{\Omega}'\ \psi(\vec{r},\ \hat{\Omega}')\sigma^{s}(\vec{r},\ \hat{\Omega}' \rightarrow \hat{\Omega}) + S \qquad (5)$$

is the "constant cross-section" approximation or the "monoenergetic" transport equation. Solutions to the monoenergetic equation are not, in general, obtainable particularly when finite boundaries or material interfaces are present. The particle flux in an infinite, homogeneous medium with an isotropic point or line source may, however, be determined in a straightforward manner. The introduction of even a simple boundary condition greatly complicates the treatment. The classical "Milne Problem" treats the infinite half-space defined by $z \geq 0$. There is a net flux in the negative z direction and the half-space $z < 0$ is taken to be a vacuum so that particles emergent at $z = 0$ cannot return. The description is roughly that of a star. The particles are photons which are produced deep within the star ($z = +\infty$) and emerge from its constant cross-section, isotropically scattering interior at ($z = 0$). The photon angular distribution at the surface may be obtained by the Wiener-Hopf method [4] and probably represents the most difficult type of problem for which an analytic solution is possible.

As exact solutions are not possible for more complex types of problems than those considered above, some of the methods which may be applied to more difficult cases will be briefly discussed. The most powerful of these is the spherical harmonics method [5] in which the integro-differential transport equation is reduced to a set of differential equations. This is done by expanding those terms of equation (5) which exhibit angular dependence in sets of orthogonal polynomials. The resulting series for each of these functions is then substituted back into the transport equation and the orthogonality property used to obtain an infinite set of differential equations in the angular flux

moments. Since there are an infinite number of equations, an exact solution is impossible. However, any degree of accuracy may be had by increasing the number of equations retained. The various moments may also be related to physical quantities in that the first moment corresponds to the scalar flux, $\phi(\vec{r})$, and the second to the particle current, $J(\vec{r}) = \int \hat{\Omega}\psi(\vec{r}, \hat{\Omega})d\hat{\Omega}$.

Retention of the first four equations in the infinite set effectively removes the angular dependence from the flux and leads to the diffusion theory approximation. This approximation is widely used in designing certain types of nuclear reactors. However, neglect of the angular dependence leads to inaccuracies near strong absorbers, material interfaces, and system boundaries. Diffusion theory is, therefor, most useful in large, relatively homogeneous reactors. There are many additional refinements which may be included in diffusion theory to extend its range of applicability. Until recently, most practical reactor analysis was accomplished through the use of computer programs designed to solve the diffusion equations. The current trend to smaller, more highly enriched, nuclear reactors has, however, necessitated the use of more accurate approximations to the transport equation.

The spherical harmonics formulation of the Boltzmann equation is capable of yielding extremely accurate results if a sufficient number of the expanded equations are retained. However, the rapid increase in the number of calculations required for the higher order terms and the difficulty encountered in treating multidimensional geometries limit its utility. Thus, while some use of the method has been made through the

application of computers, such approximations have been limited to lower order and one dimensional calculations [6].

The last method to be covered will be discussed in somewhat more detail because of its relationship to the transport methods currently used. The basic technique, known as the method of discrete ordinates, was suggested by Wick [7] and has been developed and extended by Chandrasekar [8]. As the method is restricted to one dimensional geometries, equation (5) will be used, in a form suitable for a homogeneous, isotropic medium, to illustrate the concept. Let the single coordinate be $z(\vec{r} \to z)$; the angular dependence is only on $\Omega_z(\Omega_z \to \mu)$; the scattering cross-section is independent of position and angle $[\sigma^s(\bar{r},\hat{\Omega}' \to \hat{\Omega}) \to \sigma^s]$; and, due to symmetry, the integration over μ is from -1 to +1. Equation (5) then becomes

$$\mu \frac{\partial \psi(z,\mu)}{\partial z} + \psi(z,\mu)\sigma^t = \int_{-1}^{1} \psi(z,\mu')d\mu' + S \qquad (6)$$

The major difficulty with the transport equation is caused by the presence of the integral term on the right hand side of (6). Rather than attempt to remove this term by some purely mathematical treatment, the Wick-Chandrasekar concept is based on immediately evaluating the integral through some numerical technique. Let the integral be approximated by some quadrature formula

$$\int_{-1}^{1} \psi(z,\mu')d\mu' = \sum_{n=1}^{N} b_n \psi(z,\mu_n) \qquad (7)$$

and a system of N differential equations is obtained:

$$\mu_i \frac{d\psi(z,\mu_i)}{dz} + \psi(z,\mu_i)\sigma^t(z) = \sum_{n=1}^{N} b_n \psi(z,\mu_n) \quad [n=1,2,\ldots N] \qquad (7)$$

each of which involves summation of the series approximating the integral over all N values of μ_n. This approach is of interest in that it makes direct use of a numerical integration technique to solve the transport equation. Several consequences of the method are apparent. The solution to equation (6) now consists of a set of N differential equations in N unknowns. The method is most suited for an iterative process since the calculation is simplified if a value for all μ_n is available for the determination of a μ_i. The discrete ordinates, the μ_n, may be chosen in several ways. In particular, if the $\psi(z,\mu)$ are assumed to be given by a polynomial, then a Gaussian quadrature, with the μ_n

$$\int_{-1}^{1} \psi(z,\mu)d\mu = \sum_{n=1}^{N} w_n \psi(z,\mu_n) \qquad (8)$$

based on the zeros of the Legendre polynomial of degree n+1, gives an exact result for $\psi(z,\mu)$ of degree 2n+1 or less. This treatment, while seemingly quite different, has been shown to be almost equivalent to that of the spherical harmonics method.

The prime disadvantage of the method of discrete ordinates, as applied by Wick and Chandrasekar, lies in its extension to multidimensional spatial systems. There is no derivation analogous to that of

the Gaussian quadrature for more than one spatial dimension. Therefore, while there is no bar to use of the method in such systems, it is not possible to set limits on the accuracy of the resulting solutions nor to determine, a priori, an optimum set of discrete ordinates.

The method of discrete ordinates has been applied to multidimensional systems by Carlson [9]. This treatment, the S_n method, differs basically from that of Wick-Chandrasekar in that no formal justification for the choice of the ordinates is involved. Instead, a number of points on the unit sphere defined by $\hat{\Omega}$ are specified and their weighted sum

$$\int_{d\hat{\Omega}}^{1} \psi(\vec{r},\hat{\Omega})\, d\hat{\Omega} = \sum_{n=1}^{N} w_n\, \psi_n(\vec{r},\Omega_n) \tag{9}$$

taken to approximate the integral in the transport equation. This S_n technique has proven to be quite powerful in finding solutions to general problems involving the transport equation.

CHAPTER III

THE DISCRETE ORDINATES (S_n) METHOD

Since the discrete ordinates method forms the basis of the work performed in this study, a fairly detailed presentation of the features of the method will be made [10][11][12][13]. In particular, those aspects of the technique which are subsequently altered will be emphasized in order to facilitate the discussion of the next chapter.

Although the general purpose of the discrete ordinates method is, of course, the solution of the linear Boltzmann transport equation, details of the process are more clearly understood if the derivation of the difference equations is presented directly rather than as a consequence of the application of differencing techniques to equation (3) The presentation involves the fundamental concept of the conservation of particles, along with the assumptions of Chapter I, in terms of finite differences of the variables. Although the derivation will be made as general as possible, the work performed has been based primarily on configurations having Cartesian coordinate (x,y,z) geometry and, where necessary for completeness, this geometry will be used. As the formalism used in treating the energy dependence is not directly connected with the S_n method, it will be covered in the next chapter and, for clarity, the energy subscripts omitted from the following.

Consider the three dimensional (x,y,z) geometry shown in figure 1. Let this represent a general spatial mesh cell from among those formed by superimposing a coordinate grid on the configuration to be analyzed. The mesh intervals and boundaries in each direction are $x_i(i=0,I)$, $y_j(j=0,J)$, and $z_k(k=0,K)$. There are a total of IxJxK mesh cells in the configuration. The dimensions of the cell shown in figure 1 are $\Delta x = (x_{i+1} - x_i)$, $\Delta y = (y_{j+1} - y_j)$, and $\Delta z = (z_{k+1} - z_k)$. If the center of the cell is defined to be located at $x_{i+1/2}$, $y_{j+1/2}$, $z_{k+1/2}$, then the volume is given by $V_{i+1/2,j+1/2,k+1/2} = \Delta x\, \Delta y\, \Delta z$. The area of the cell face in the y-z plane is denoted by $A_{i,j+1/2,k+1/2} = \Delta y\, \Delta z$, and similarly for the other faces in the x-z, $B_{i+1/2,j,k+1/2} = \Delta x\, \Delta z$ and x-y, $C_{i+1/2,j+1/2,k} = \Delta x\, \Delta y$ planes.

In figure 2 is shown the first octant of the unit sphere defined by $\hat{\Omega}$. The discrete ordinates values to be used in the transport equation integral may be thought of as points on the unit sphere with origin at (0,0,0). Let there be M such points with the corresponding angular flux denoted by $\psi_m(m=1,M)$. The average value of the angular flux in each mesh interval for each direction, in accord with the convention established above is $\psi_{m,i+1/2,j+1/2,k+1/2}$. There are IxJxKxM values for this quantity and, to avoid confusion, these will always be denoted by $\underline{\psi}$. Each m point is fully specified by giving the direction cosines (μ,η,ξ) with respect to the x, y, and z axes. The law of direction cosines must hold so that, for each point:

$$\mu_m^2 + \eta_m^2 + \xi_m^2 = 1.0$$

As shown by equation (9), there is a weight associated with each point

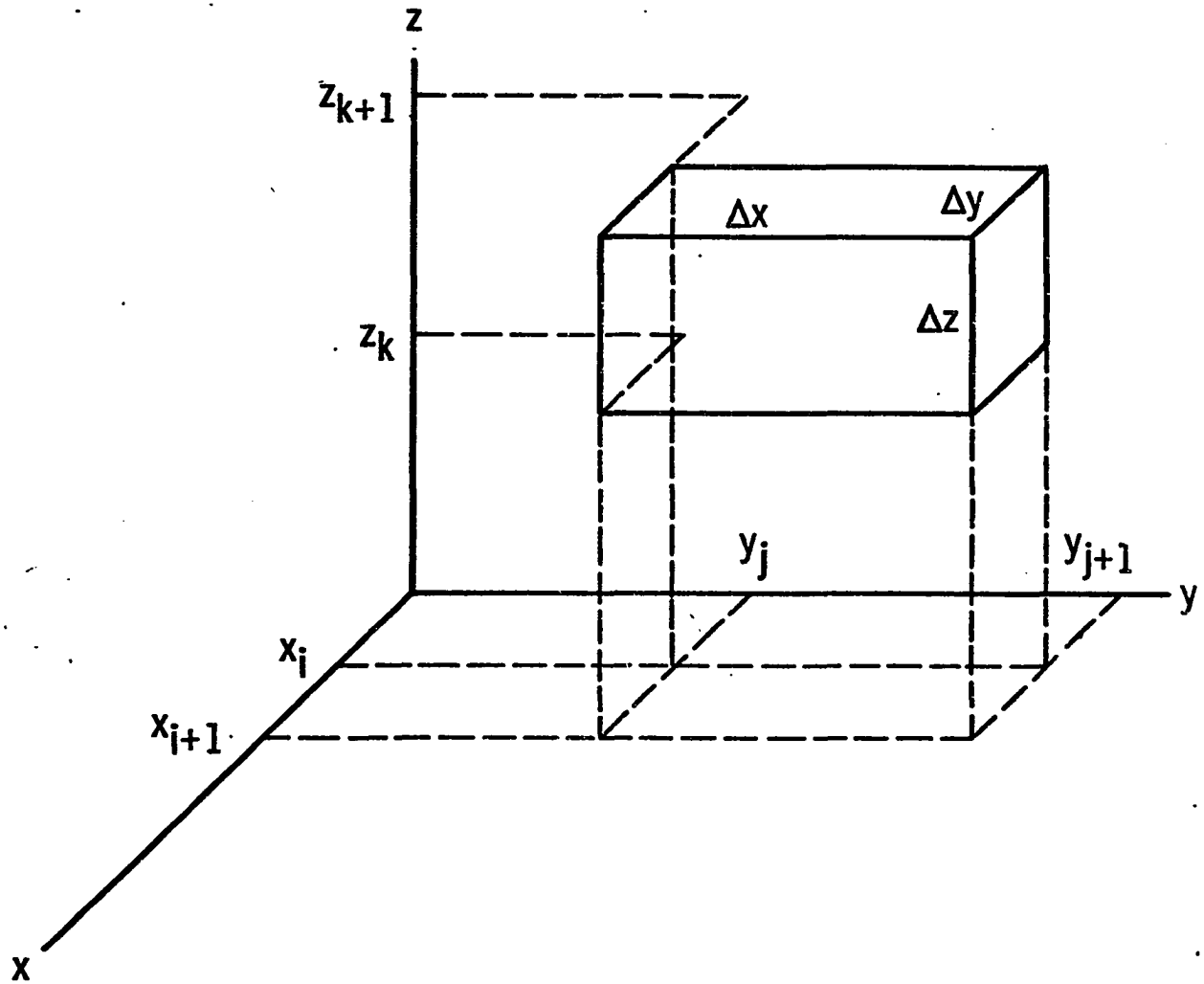

Figure 1. - Rectangular coordinate mesh cell.

1. $\psi(\Omega_m)$ represents the angular flux between the directions m - 1/2, m + 1/2.
2. The intersection of lines of constant (μ, η, ξ) determines each direction.

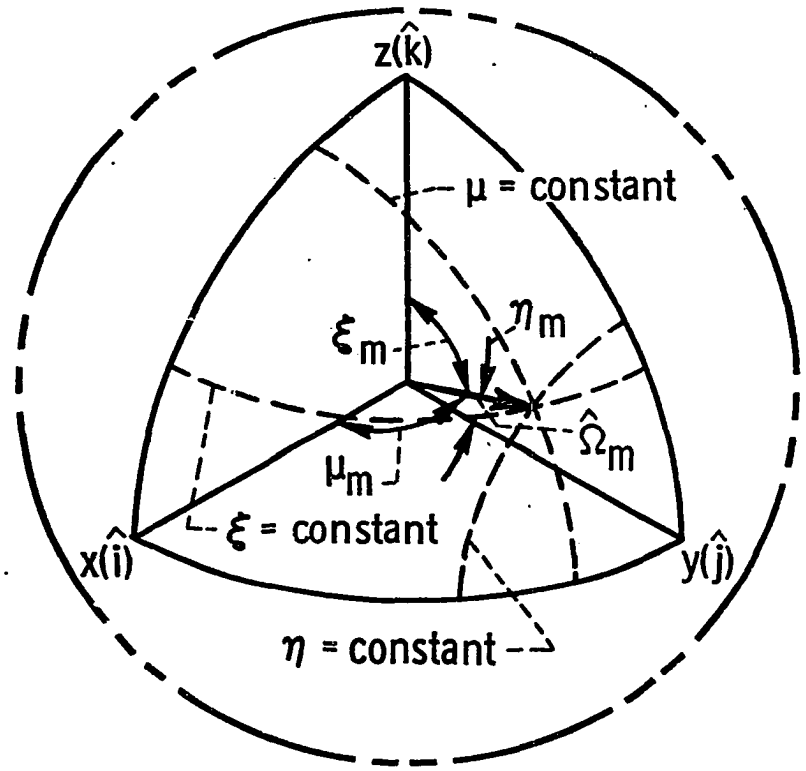

Figure 2. - Unit direction vector coordinates.

$\hat{\Omega}_m = (\mu_m, \eta_m, \xi_m)$. These weights must sum to the area of the unit sphere but are given in units of 4π so that a condition on the w_m is

$$\sum_{m=1}^{M} w_m = 1.0$$

Then, by equation (9), the scalar flux is

$$\varphi = \sum_{m=1}^{M} w_m \underline{\psi}_m \tag{10}$$

Although the weights may be arbitrarily assigned, subject to the above restriction, the most consistent set is obtained when each weight is associated with that portion of the unit sphere surface associated with its corresponding direction.

Using the definitions and subscript conventions above, the rate of change of the neutron density, $n = \psi/v$, between times t_{s+1} and t_s, for the direction range m in the cell of figure 1 may be written as

$$\frac{w_m}{v}\left[\underline{\psi}_{s+1,m,i+1/2,j+1/2,k+1/2} - \underline{\psi}_{s,m,i+1/2,j+1/2,k+1/2}\right)V_{i+1/2,j+1/2,k+1/2}\Bigg] \tag{11}$$

The number of neutrons crossing a cell face is the product of the angular flux at the cell surface, the cosine of the angle between the surface normal and the neutron direction, and the cell surface area. For the same direction, m, the flow into the cell through the i, j, and k faces is

$$w_m \mu_m A_{i,j+1/2,k+1/2} \psi_{s+1/2,m,i,j+1/2,k+1/2} \Delta t$$

$$+ w_m \eta_m B_{i+1/2,j,k+1/2} \psi_{s+1/2,m,i+1/2,j,k+1/2} \Delta t \qquad (12)$$

$$+ w_m \xi_m C_{i+1/2,j+1/2,k} \psi_{s+1/2,m,i+1/2,j+1/2,k} \Delta t$$

Again, for direction m, the flow out through the i+1, j+1, and k+1 faces is

$$w_m \mu_m A_{i+1,j+1/2,k+1/2} \psi_{s+1/2,m,i+1,j+1/2,k+1/2} \Delta t$$

$$+ w_m \eta_m B_{i+1/2,j+1,k+1/2,} \psi_{s+1/2,m,i+1/2,j+1,k+1/2} \Delta t \qquad (13)$$

$$+ w_m \xi_m C_{i+1/2,j+1/2,k+1} \psi_{s+1/2,m,i+1/2,j+1/2,k+1} \Delta t$$

For the present, let the number of source neturons produced in the cell per unit direction, per unit time, and per unit volume be $S_{s+1/2,m,i+1/2,j+1/2,k+1/2}$. Then the number of neutrons generated in the cell is

$$w_m S_{s+1/2,m,i+1/2,j+1/2,k+1/2} V_{i+1/2,j+1/2,k+1/2} \Delta t \qquad (14)$$

which includes neutrons scattered into the direction m. The number of neutrons removed from the cell by all collision processes is the product of the average flux, the angular area, the cell volume, and the time interval

$$w_m \sigma^t_{s+1/2,i+1/2,j+1/2,k+1/2} \psi_{s+1/2,m,i+1/2,j+1/2,k+1/2} V_{i+1/2,j+1/2,k+1/2} \Delta t \qquad (15)$$

Equating the rate of change in neutron density to the remainder of these terms, dropping the central subscripts, and dividing by $w_m \Delta t$ yields

a neutron balance equation for the finite cell:

$$\frac{(\psi_{s+1} - \psi_s)V}{v\,\Delta t} = \mu(A_i\psi_i - A_{i+1}\psi_{i+1}) + (B_j\psi_j - B_{j+1}\psi_{j+1})$$

$$+ \xi(C_k\psi_k - C_{k+1}\psi_{k+1}) + SV - \sigma^t\psi V \qquad (16)$$

Using the definitions of the various surface areas and the volume, dividing through by $\Delta x\,\Delta y\,\Delta z$ yields:

$$\frac{\Psi_{s+1} - \Psi_s}{v\,\Delta t} = \frac{\mu(\psi_{i+1} - \psi_i)}{\Delta x} + \frac{\eta(\psi_{j+1} - \psi_j)}{\Delta y} + \frac{\xi(\psi_{k+1} - \psi_k)}{\Delta z} + \sigma^t\psi = S \qquad (17)$$

or in the limit,

$$\frac{1}{v}\frac{\partial\psi}{\partial t} + \mu\frac{\partial\psi}{\partial x} + \eta\frac{\partial\psi}{\partial y} + \xi\frac{\partial\psi}{\partial z} + \sigma^t\psi = S \qquad (18)$$

which is the three dimensional rectangular coordinate representation of the transport equation (2). Extension of the derivation to other geometries is relatively straightforward.

All the terms in equation (16), with the exception of S are precisely rendered. In order to obtain a more specific description of this source term, assume that equations (16) and (17) represent not the monoenergetic problem but some specified energy range, ΔE, and that their energy dependence exterior to this range is governed by similar equations. The source terms, $S(\Delta E)$, may then be separated into three components: external sources, fission sources, and scattering sources. The external sources include those due to particle accelerators and neutron producing materials. They correspond to those grouped into the extraneous source term under (1) of Chapter I and lead to the

non-homogeneous equation mentioned there. In general, these source strengths are known and may be put directly into the calculation. It is, therefore, sufficient to denote them by

$$Q(\Delta E)_{s+1/2,m,i+1/2,j+1/2,k+1/2}$$

which has dimensions of neutrons per unit time, per unit direction, per unit volume.

The remaining components are proportional to the neutron flux. The fission source results from the interaction of a neutron with a fissionable nucleus. According to the definition of Chapter I, the reaction rate for the fission process is proportional to the scalar neutron flux

$$F_f(E) = \phi(E)\sigma^f(E)$$

The mean number of neutrons per fission, which may be energy dependent, is usually denoted by $\nu(E)$ so that the total number of neutrons produced is given by

$$F(E) = \int_E \nu(E)\sigma^f(E)\phi(E)dE$$

These neutrons may be emitted at various energies. If $X(E)$ is defined as the fission spectrum, or normalized probability that a neutron appear at energy E, the number of neutrons produced by the fission process in the range ΔE is

$$F(\Delta E) = X(\Delta E) \int_E \nu(E)\sigma^f(E)\phi(E)dE$$

The collision source for the energy range ΔE is the product of the scattering reaction rate at all other energies and the probability that a scattered neutron will emerge in ΔE. It will be assumed that this scattering distribution function is known since it is a property of the medium. The inscattering source term then consists of

$$SI(\Delta E) = \int_E \sigma^s(E \to \Delta E)\phi(E)dE$$

The total source, S, is the sum of these three terms.

Since it is primarily desired to solve the time-independent transport equation, equation (16) becomes

$$\mu(A_{i+1}\psi_{i+1} - A\psi_i) + \eta(B_{j+1}\psi_{j+1} - B_j\psi_j) + \xi(C_{k+1}\psi_{k+1} - C_k\psi_k)$$

$$+ \sigma^t\psi V = SV \qquad (19)$$

Equation (19), representing the three dimensional transport equation in rectangular coordinates, is now in a form amenable to numerical calculation. There are, however, seven unknowns, not including the scalar fluxes appearing in the source terms, in this equation. These unknowns are the angular fluxes at six faces of the rectangular parallelopiped enclosing the volume V and the average angular flux of equation (15). Three of these angular fluxes are known as a result of the boundary conditions placed on the configuration. The rest must be specified by the introduction of some relationship between the various angular fluxes. Since the main body of the calculation is concerned with the repeated determination of the angular fluxes over the spatial mesh, it is preferable to use a physical model which is as simple as possible. Two such

relationships are currently used:

(1) The Step Model

In the step model it is assumed that each of the unknown angular fluxes at the opposite cell boundaries is equal to the central average angular flux:

$$\underline{\psi} = \psi_i = \psi_j = \psi_k \tag{20}$$

(2) The Diamond Model

In the diamond model the unknown boundary angular fluxes are assumed to have an average value, $(\psi_{i+1} + \psi_i)/2$ equal to the central average angular flux:

$$\psi_{i+1} + \psi_i = \psi_{j+1} + \psi_j = \psi_{k+1} + \psi_k = 2\underline{\psi} \tag{21}$$

It is seen that knowledge of the three boundary angular fluxes, either from the boundary conditions imposed or from calculation of the previous adjacent mesh cells, plus either of the above relations (20) or (21) changes the form of equation (19). For the diamond model, for example, if the ψ_i, ψ_j, ψ_k are given, equation (21) yields for the central average angular flux:

$$\underline{\psi} = \frac{\mu(A_{i+1} + A_i)\psi_i + \eta(B_{j+1} + B_j)\psi_j + \xi(C_{k+1} + C_k)\psi_k + SV}{2\mu A_{i+1} + 2\eta B_{j+1} + 2\xi C_{k+1} + \sigma^t V} \tag{22}$$

in terms of the known angular fluxes. The opposite boundary fluxes are then also found by equation (21)

$$\begin{aligned} \psi_{i+1} &= 2\underline{\psi} - \psi_i \\ \psi_{j+1} &= 2\underline{\psi} - \psi_j \\ \psi_{k+1} &= 2\underline{\psi} - \psi_k \end{aligned} \tag{23}$$

so that the resulting system of equations involves three unknowns in three equations. It should also be noted that there is a similar set of equations (19), (22), and (23) for every characteristic direction, m, used in the angular quadrature. The essential feature of the derivation of equation (22) is that the value of the source term in the numerator for some energy range, ΔE, requires a knowledge of the fluxes at all other energies. This was shown in the previous discussion of the inscattering and fission sources where each of these terms was taken to be proportional to the scalar flux. Thus, solution of the general form of equation (22) must constitute an iterative process. A further discussion of the nature and treatment of these sources will be reserved for the next chapter.

It is now possible to describe the flow of the discrete ordinates calculation. For simplicity, a two dimensional rectangular coordinate illustration will be used. It is shown in figure 3 and has three spatial mesh intervals along each of the I and K axes for a total of (IxK) nine intervals. Let the angular quadrature consist of only one direction in each quadrant. There is then a total of four directions, M=4, along which the angular fluxes must be determined. Assume that an initial estimate of the scalar flux is made, to allow calculation of the source terms, and that the boundary conditions are known. The form of the boundary conditions is usually such that the initial behaviour of the angular fluxes is specified. For example, a "vacuum" or "no return current" condition states that the incident angular flux along all characteristic directions at that boundary is zero. The subscript conventions used in equation (11) will be followed. Thus

1. The ψ are angular fluxes at the spatial mesh interfaces.
2. The $\underline{\psi}$ are angular fluxes centered with respect to all differenced variables.
3. Circle in IK = 5 indicates order in which directions are executed.

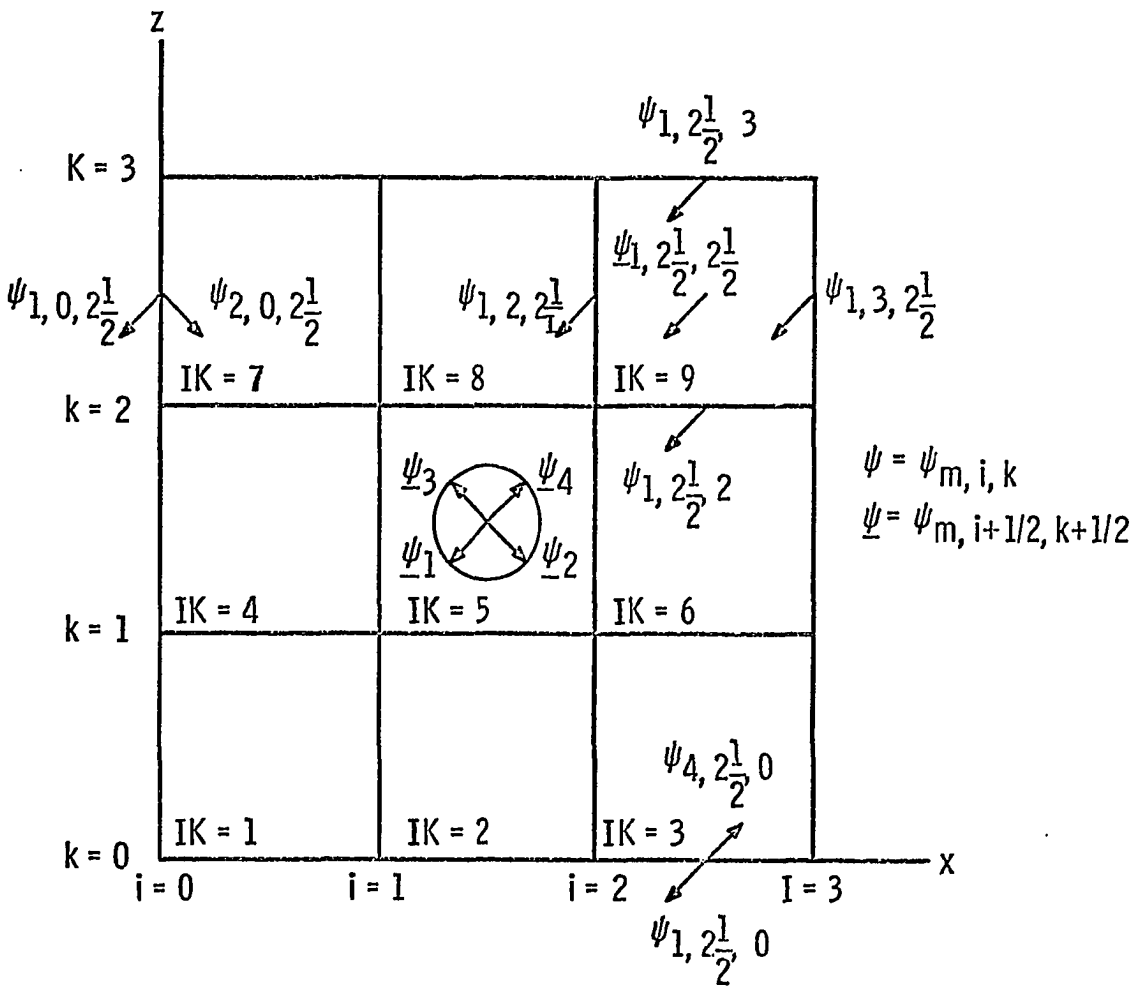

Figure 3. - Angular-spatial quadrature flow diagram.

$\psi_{m,i,k} = \underline{\psi}_{m,1+1/2,1+1/2}$ denotes the central average angular flux in the mesh interval bounded by i=1, i=2, k=1, and k=2. The characteristic directions are numbered in the order used as indicated in the same figure.

The calculation is begun by using the known values (from the boundary conditions) of $\psi_{1,2-1/2,3}$ and $\psi_{1,3,2-1/2}$ in equation (22) to determine $\underline{\psi}_{1,2-1/2,2-1/2}$ in the mesh interval IK=9. Equations (23) then give values for $\psi_{1,2-1/2,2}$ and $\psi_{1,1-1/2,2}$. The central average angular flux for interval IK=8 may then be found and, consequently, the angular fluxes at the surrounding mesh interfaces. At the left hand boundary of the configuration, the appropriate conditions are applied and the $\psi_{2,i,j}$ for the top row found for the direction m=2. The calculation then proceeds down to the middle row and, using the now known $\psi_{1,i+1/2,2}$ sweeps from right to left and back. When the bottom row is fully determined for the $\psi_{1,i+1/2,0}$ and $\psi_{2,i+1/2,0}$, an upward sweep is performed to complete the angular flux array by finding $\psi_{3,i,j}$ and $\psi_{4,i,j}$. All the angular fluxes required for the whole mesh sweep are then known. Each such complete sweep, or pass, is an "inner" iteration. Figure 3 shows only the fluxes necessary for the foregoing description. The whole angular flux array comprises the four angular fluxes at each mesh interface and four central average angular fluxes in each mesh interval. Only the mesh interval IK=5 in the figure shows the complete array. After each complete inner iteration, the scalar flux in each interval is revised using

$$\varphi = \sum_{m=1}^{4} w_m \underline{\psi}_{m,i+1/2,k+1/2} \qquad (10)$$

When the inner iterations have converged, (i.e., when the angular fluxes do not vary by more than some specified convergence criteria) the resulting scalar fluxes are used to update, or recalculate, the various source terms. This process is done in an "outer" iteration. The steps in reaching a solution may be summarized: Using an initial scalar flux estimate, the source terms for the first group are found. The angular fluxes are then converged by performing the required number of inner iterations. The scalar fluxes and source terms are updated in the outer iteration and the whole process, of inner and outer iteration, continued until final convergence on either, or both, the angular and scalar fluxes is attained. In a standard S_n calculation, the procedure is identical for all geometries (with the appropriate changes in the areas and volumes) and types of discrete ordinates. It is evident that direct application of equations (16) or (17) in this manner affords one method for solving the time dependent transport equation. The times, t_{s+1} and t_s may be considered merely other "discrete ordinates" and the solution obtained for each time step.

Various convergence tests and techniques for accelerating convergence are utilized in the discrete ordinates approximation. The methods presented in the following Chapter are meant to be fully compatible with these existing techniques and to be used in conjunction with them if so desired.

CHAPTER IV

QUADRATURE VARIATIONS

Solutions to the general stationary transport equation

$$\hat{\Omega} \cdot \nabla\psi(\bar{r},E,\hat{\Omega}) + \psi(\bar{r},E,\hat{\Omega})\sigma^{t}(\bar{r},E)$$

$$= \int dE'd\hat{\Omega}'\psi(\bar{r},E',\hat{\Omega}')\Sigma^{s}(\bar{r},E' \rightarrow E,\hat{\Omega}' \rightarrow \Omega) + S(\bar{r},E,\hat{\Omega}) \quad (3)$$

are, at present, available only through recourse to numerical methods [14]. Of the methods which have been attempted, the discrete ordinates approximation presented in the preceding chapter has proven most satisfactory. The application of this method, particularly to complex spatial configurations requiring high order angular quadratures, is restricted by several factors. The single most important limitation on the method is the extremely large amount of calculational effort required to solve detailed multidimensional problems. An ancillary problem, which is partially a consequence of using lower order angular quadratures in an attempt to simplify the calculation, is the return of incorrect particle flux distributions. That is, although the choice of a spatial mesh is relatively simple since the physical composition of the configuration is known in advance, selection of the angular quadrature set is more difficult since the behaviour of the angular fluxes is not known prior to the calculation.

In this chapter, several methods are to be presented which remove or minimize some restrictions inherent in applications of the discrete ordinates approximation. In addition, some aspects of these methods may be utilized to allow extension of the approximation to classes of problems not previously susceptible to calculation.

Machine Solutions

In implementing these methods, it is necessary to use high speed digital computers to obtain solutions to the discrete ordinates approximations to the transport equation. In making comparisons between the methods to be presented and the standard S_n techniques, considerable care has been taken to assure that the computer hardware and software were identical for all calculations. The standard multidimensional S_n program is quite complex although there is little variation in programming between different machine codes [15][16]. In the results presented all operations other than those directly involved in the work performed conform to the standard treatment. The conclusions drawn, are, therefore, intended to be applicable to the general discrete ordinates method and not dependent on either machine equipment or programming techniques.

In the preceding chapter, it was noted that application of spatial and angular differencing techniques to the transport equation led to equation (22). This equation, as formulated, applies strictly only to the angular flux distribution. In deriving the various source terms, SV, grouped in the equation, only the scalar fluxes were used. This is possible since the reaction rate for the scattering and fission processes

is presumed independent of the incident angle of the neutron. The general flow of the inner and outer iterations previously mentioned may then be arranged as follows: In the inner iteration, only the angular fluxes are calculated. The set of these angular fluxes in the energy range ΔE allows the summation of equation (10) to be performed to obtain the scalar flux in ΔE. This revised scalar flux may then be used to revise the scattering source term but only in the range ΔE. The scalar fluxes and, consequently, all other source terms at different energies remain unchanged. It is most convenient to treat these terms at one time in the outer iterations. Therefore, subsequent use of the terms inner iteration and outer iteration may be inferred to be synonymous with, respectively, the angular and scalar flux calculations. The computer program procedure is then, in the inner iterations, to determine the angular fluxes in ΔE, revise the scattering source in ΔE, and repeat this calculation until the angular fluxes converge. When the whole energy range of the problem has been so treated, the total scalar flux distribution is used, in the outer iterations, to revise the source terms. The whole procedure is reiterated until both the angular and scalar fluxes are converged. The formal mathematical operations involved in rendering the transport equation amenable to numerical analysis will be presented below. A matrix notation will also be introduced to simplify discussion of the various methods.

Scalar and Angular Flux Matrices

In the general, energy dependent transport equation, the energy dependence may be effectively removed by use of the multigroup

formalism [17]. In this process, all energy dependent quantities are replaced by flux weighted averages over the desired energy ranges. For example, the value of any energy dependent quantity, f(E), to be used in energy group g is defined as

$$\bar{f}_g = \frac{\int_{\Delta E} f(E)\phi(E)dE}{\int_{\Delta E} \phi(E)dE}$$

where ΔE is the energy range of the group. Since a knowledge of the true scalar flux, $\phi(E)$, would constitute a solution to the problem to be solved, and is not available, some estimate of this quantity must be made. Many averaging techniques are possible but all are based on solving the transport equation in an infinite medium similar to that of the actual configuration. Since averaging over smaller energy groups may be expected to incur less error, the accuracy of solutions to the transport equation will generally increase with the number of energy groups.

If these energy averaged quantities are used in equation (3), a set of partial differential equations, similar in form to the original equation

$$\hat{\Omega} \cdot \nabla\psi_g(\vec{r},\hat{\Omega}) + \psi_g(\vec{r},\hat{\Omega})\sigma_g^t(\vec{r}) = S_g(\vec{r},\hat{\Omega}) \qquad g=1,\ldots G \tag{24}$$

is obtained. These equations are coupled only by the particle source terms, $S(\vec{r},\hat{\Omega})$, which include extraneous, fission, and inscattering sources. The extraneous sources are taken to be those which are not

functions of the flux and are presumed to be specified:

$$Q_g(\bar{r},\hat{\Omega}) \tag{24a}$$

Following the arguments of chapter III, the multigroup representation of the fission source is:

$$\frac{\chi_g}{\lambda}\sum_{g'=1}^{G}\nu\sigma^f_{g'}(\bar{r})\left[\frac{1}{4\pi}\int_{\hat{\Omega}'}\psi_{g'}(\bar{r},\hat{\Omega}')d^2\hat{\Omega}'\right] \tag{24b}$$

where λ is a normalization factor required because of the variation in flux level due to neutron multiplication in the assembly. It is, of course, also the principle eigenvalue of the assembly since it yields the flux distribution which is everywhere positive. The quantity $1/\lambda$ is the effective multiplication factor or ratio of the neutron production in the n^{th} iteration to that of the $(n-1)^{th}$ iteration. The inscattering source, including the within group, or $(g \to g)$, contribution is:

$$\sum_{g'=1}^{G}\frac{1}{4\pi}\int_{\hat{\Omega}'}\sigma^s_{g'\to g}(\vec{r},\hat{\Omega}' \to \hat{\Omega})\psi_{g'}(\vec{r},\hat{\Omega}')d^2\hat{\Omega}' \tag{24c}$$

where $\sigma^s_{g'\to g}$ is the kernel for scattering from group g' to g through the angle $\cos^{-1}(\hat{\Omega}' \cdot \hat{\Omega})$. The total source of equation (24) is then the sum of whichever of these three terms exits in a given instance.

Since, in theory, all groups may contribute to each other, the system comprises a set of G linear partial differential equations

in G unknowns. These multigroup equations are operated on primarily in the outer iterations. Although the system of equations (24)

$$\left\{\hat{\Omega}\cdot\nabla\psi_g(\vec{r},\hat{\Omega})+\psi_g(\vec{r},\hat{\Omega})\sigma_g^t(\vec{r})=Q_g(\vec{r},\hat{\Omega})\right.$$
$$+\frac{\chi_g}{\lambda}\sum_{g'=1}^{G}\nu_{g'}\sigma_{g'}^t(\vec{r})\left[\frac{1}{4\pi}\int_{\hat{\Omega}'}\psi_{g'}(\vec{r},\hat{\Omega}')d\hat{\Omega}'\right] \qquad (24d)$$
$$\left.+\sum_{g'=1}^{G}\frac{1}{4\pi}\int_{\hat{\Omega}'}\sigma_{g'\to g}^s(\vec{r},\hat{\Omega}'\to\hat{\Omega})\psi_{g'}(\vec{r},\hat{\Omega}')d\hat{\Omega}\right\}$$

involves both angular and scalar fluxes, it is, as stated previously, most convenient to treat each separately. Assume that a scalar flux estimate is given to begin the calculation. The source terms appearing in equation (22), which constitute the right hand side of equation (24d), may then be determined in the following manner: The extraneous source term, $Q_g(\vec{r},\hat{\Omega})$, is given explicitly. If it is scalar, it may be inserted into the calculation at this point. If it is angularly dependent, it may be added during the course of the angular flux calculation which is to be subsequently discussed. Since neither option presents any difficulties, the extraneous sources need not be further considered. The integral appearing in the fission source term is merely the scalar flux and this may be multiplied by the group constants shown to obtain the fission source contribution. A full treatment of the scattering source term complicates discussion of the calculation and is not required for the work performed in this study. If the scattering process is assumed to be isotropic, then the scattering source is the product of the scalar flux and the elastic

scattering matrix which, since it is a property of the target medium, is presumed specified. Under these conditions, the scalar fluxes may be used to obtain the source terms for each energy group. Let the total group source be S_g. Dropping unnecessary subscripts and noting that

$$\int_{\hat{\Omega}'} \psi_g(\vec{r},\hat{\Omega}')d\hat{\Omega} = \phi(\vec{r})$$

yields, from the right hand side of equation (24d),

$$S_g = \frac{\chi_g}{\lambda}\left[\nu_1\sigma_1^f\phi_1 + \nu_2\sigma_2^f\phi_2 + \nu_3\sigma_3^f\phi_3 + \cdots\right]$$
$$+ \phi_1\left[\sigma^s_{1\to1} + \sigma^s_{1\to2} + \cdots\right] + \phi_2\left[\sigma^s_{2\to1} + \sigma^s_{2\to2} + \cdots\right]$$
$$+ \cdots$$

for those fission and scatter terms which contribute to group g. The coefficients of each group scalar flux, from the above equation, may be collected. If these are represented by $s_{gg'}$, the following set of equations is obtained for the group sources:

$$S_1 = s_{11}\phi_1 + s_{12}\phi_2 + s_{13}\phi_3 + \cdots$$
$$S_2 = s_{21}\phi_1 + s_{22}\phi_2 + s_{23}\phi_3 + \cdots$$
$$\vdots$$

or, in matrix notation,

$$|\mathcal{S}|\,\overline{\phi} = \overline{S} \qquad (25)$$

where $|\mathcal{S}|$ will be referred to as the scalar flux matrix and $\overline{\phi}$ and $\overline{S}$ are, respectively, the energy group dependent scalar flux and source vectors.

Introduction of the discrete ordinates approximation, through equations (19) and (22) of the preceding chapter, shows that the governing equation within each energy group consists of a set of equations of the form (22) with, however, the direction cosines, μ, η, and ξ, varying for each characteristic direction and the mesh interval dimensions, A, B, and C, varying for each spatial position. Using equation (23), determination of the angular fluxes then requires a set of three equations in three unknowns:

$$\begin{aligned} \psi_{m,i+1} &= 2\underline{\psi}_{m,\bar{i},\bar{j},\bar{k}} - \psi_{m,i} \\ \psi_{m,j+1} &= 2\underline{\psi}_{m,\bar{i},\bar{j},\bar{k}} - \psi_{m,j} \\ \psi_{m,k+1} &= 2\underline{\psi}_{m,\bar{i},\bar{j},\bar{k}} - \psi_{m,k} \end{aligned} \tag{23}$$

where $\underline{\psi}_{m,\bar{i},\bar{j},\bar{k}}$, the central average angular flux, is given by equation (22). In the general form of equation (22) for each energy group

$$\underline{\psi}_{m,\bar{i},\bar{j},\bar{k}} = \frac{\mu_m(A_{i+1} + A_i) + \eta_m(B_{j+1} + B_j) + \xi_m(C_{k+1} + C_k) + S_{i,j,k}V_{i,j,k}}{2\mu_m A_{i+1} + 2\eta_m B_{j+1} + 2\xi_m C_{k+1} + \sigma^t_{i,j,k}V_{i,j,k}} \tag{22}$$

all the quantities on the right hand side of the equation, but for the scalar fluxes involved in the source terms, S, may be regarded as known from the calculation of the previous mesh interval. If the terms containing the direction cosines in the numerator of equation (22) are represented by K^1 and the coefficient of the source term by K^2, then the equation for each energy group may be written

$$\underline{\psi}^g = K^{1g} + K^{2g}S^g \tag{26}$$

The source terms, by equations (24), are functions of the scalar

fluxes in all energy groups. Introduction of equation (25) into equation (26) yields

$$\underline{\psi}^g = K^{1g} + K^{2g}|\mathcal{J}^g|\bar{\phi} \qquad (27)$$

where all quantities are functions of m, i, j, and k. Performing the indicated multiplication (only one row of the $|\mathcal{J}|$ matrix is directly involved) leads to an equation of the form

$$\underline{\psi}^g = K^{1g} + K^{2g}\left[s_{g1}\phi_1 + s_{g2}\phi_2 + \cdots\right] \qquad (27a)$$

If the terms containing all the scalar fluxes but those in group g are combined with the $K^{1,g}$ to form another constant, $K^{3,g}$, this equation becomes

$$\bar{\psi}_g = K^{3g} + s_{gg}\phi_g \qquad (27b)$$

which, as a consequence of equation (10), may also be written as

$$\underline{\psi}^g = K^{3g} + s_{gg}\left[\sum_m w_m \underline{\psi}^g_m\right] \qquad (28)$$

If all terms involving the $\underline{\psi}$, with the exception of $\underline{\psi}_m$, are presumed known from the previous inner iteration, and incorporated into a new constant K, this may also be written as

$$\underline{\psi}^g_m = K + a_{gg}\underline{\psi}_m \qquad (28a)$$

where the s_{gg} and the w_m have also been combined to form a_{gg}. Since every characteristic direction, m, yields a set of equations (28a) for each permutation of i, j, and k, the angular flux equations constitute an extremely large set. Rather than write these explicitly, a matrix form will again be employed to represent the angular flux equations.

$$\overline{\psi} = |a|\ \overline{\psi} + K \tag{28b}$$

where $|a|$ will be termed the angular flux matrix.

Some additional consideration of the details of the numerical method used in obtaining solutions to the discrete ordinates approximation is now possible. In practice, it is most efficient to solve the system of equations (25) and (28). The steps in the iterative procedure are as follows: Given a scalar flux estimate, the fission and scattering source terms may be calculated using equation (25). These group source terms may now be used in equation (28) to solve for the angular fluxes in a given group. Within this group, the angular flux array thus obtained allows, through equation (10), re-calculation of the scalar fluxes in that group. These new group scalar fluxes may then be used to improve the estimate of the within group source terms and, consequently, to again determine the angular flux array. When this sequence has been completed, the resulting improved scalar fluxes may be again used in equation (25) to improve the source term estimates.

Matrix Application

According to equation (25) the multigroup discrete ordinates equations constitute a set of G linear equations which may be written in general form as

$$|A|\ \overline{\phi} = \overline{S} \tag{25}$$

where S is the total source term.

The ensuing discussion will be primarily concerned with the details of the actual numerical calculation. Use of the general matrix form, equation (25) will, however, simplify the presentation. All the methods to be presented concern alterations to the form of the matrices $|A|$ and $|a|$ or to the manner in which they are applied. Since the

general form is used, the specific matrix involved will be designated when one of the methods is developed.

Application of the definition of matrix addition to equation (25) will return a slightly different form for the matrix equation. The matrix $|\mathcal{S}|$, which represents a set of G equations in G unknowns, is a square matrix. Any square matrix may be decomposed into the sum of three related matrices

$$|\mathcal{S}| = |\mathcal{D}| + |\mathcal{L}| + |\mathcal{U}|$$

where $|\mathcal{D}|$ is a diagonal matrix, $|\mathcal{U}|$ an upper triangular matrix, and $|\mathcal{L}|$ a lower triangular matrix as indicated below

$$\begin{vmatrix} s_{11}s_{12} \cdots s_{1m} \\ s_{21}s_{22} \cdots \\ \cdot \\ \cdot \\ \cdot \\ s_{n1} \cdots s_{nm} \end{vmatrix} = \begin{vmatrix} s_{11} 0 \cdots 0 \\ 0\ s_{22} \cdots 0 \\ \cdot \\ \cdot \\ \cdot \\ 0 \cdots s_{nm} \end{vmatrix} + \begin{vmatrix} 0 \cdots 0 \\ s_{21} 0 \cdots 0 \\ s_{31}s_{32} 0 \cdots 0 \\ \cdot \\ \cdot \\ \cdot \\ s_{n1} \cdots s_{nm-1} 0 \end{vmatrix} + \begin{vmatrix} 0\ s_{12} \cdots s_{1m} \\ 0\ 0 \\ \cdot \\ \cdot \\ \cdot \\ 0 \cdots s_{n-1m} \\ 0 \cdots 0 \end{vmatrix} \tag{29}$$

therefore

$$|\mathcal{A}|\,\bar{\phi} = \left\{|\mathcal{B}| + |\mathcal{L}| + |\mathcal{U}|\right\}\bar{\phi} = \bar{S} \tag{30}$$

and premultiplication by $\mathcal{B}^{-1}$ yields

$$\bar{\phi} = -|\mathcal{B}^{-1}|\left(|\mathcal{L}| + |\mathcal{U}|\right)\bar{\phi} + |\mathcal{B}^{-1}|\,\bar{S}$$

$$\bar{\phi} = |\mathcal{A}'|\,\bar{\phi} + \bar{S}' \tag{31}$$

where

$$|\mathcal{A}'| = -\left[|\mathcal{B}^{-1}|\left(|\mathcal{L}| + |\mathcal{U}|\right)\right] \quad \text{and} \quad |S'| = |\mathcal{B}^{-1}|\,\bar{S}$$

Equation (25) is now of the same form as equation (28) with the source terms operated on only by the diagonal matrix.

Since both the scalar (31) and angular (28) flux equations involve a prior knowledge of the neutron sources, which depend on the scalar fluxes, solution of the matrix problem is an iterative procedure. Any iterative method must involve some rule for operating on an approximate solution, ϕ^{k-1}, to obtain an improved solution, ϕ^{k}. This rule will be represented by

$$\bar{\phi}^{k} = |\mathcal{M}|\,\bar{\phi}^{\,k-1} + \bar{m} \tag{32}$$

Thus, a given estimate, $\bar{\phi}^{k-1}$, will be operated on by $|\mathcal{M}|$ to obtain the improved estimate. In the multigroup equations (24), determination of the fluxes in group g involves knowledge of the fluxes in all groups $\phi_{g'<g}$ and $\phi_{g'>g}$. Since the flow of the calculation is from group g to $g+1$, the values for $\phi^{k}_{g'<g}$ are available while group g is being solved. For groups $g'>g$ only the $\phi^{k-1}_{g'>g}$ are available. For example,

in a three energy group case as stated by equation (29), prior to the k^{th} iteration

$$\begin{aligned} s_{11}\phi_1^{k-1} + s_{12}\phi_2^{k-1} + s_{13}\phi_3^{k-1} &= S_1 \\ s_{21}\phi_1^{k-1} + s_{22}\phi_2^{k-1} + s_{23}\phi_3^{k-1} &= S_2 \\ s_{31}\phi_1^{k-1} + s_{32}\phi_2^{k-1} + s_{33}\phi_3^{k-1} &= S_3 \end{aligned} \tag{33}$$

shows that in solving the first equation, only terms in the diagonal matrix, $|\mathcal{D}|$, operate on the ϕ_1 component of $\bar{\phi}$. Solution of this equation yields the improved value ϕ_1^k. In the second equation of (33), only the diagonal matrix is again involved with ϕ_2, and only the lower matrix, $|\mathcal{L}|$, operates on ϕ_1^k. The same scheme is followed in any such set of equations: only the diagonal terms are used in determining $\phi_{g'=g}$, only the lower matrix is used on $\phi_{g'<g}^k$, and the upper matrix operates only on the $\phi_{g'>g}^{k-1}$. Then equation (30) may be written

$$\left(|\mathcal{D}| + |\mathcal{L}|\right)\bar{\phi}^k = -|\mathcal{U}|\bar{\phi}^{k-1} + \bar{S}$$

or, introducing the iterative scheme of equation (32)

$$\bar{\phi}^k = -\left(|\mathcal{D}| + |\mathcal{L}|\right)^{-1}|\mathcal{U}|\phi^{k-1} + \left(|\mathcal{D}| + |\mathcal{L}|\right)^{-1}\bar{S} \tag{34}$$

The most recently calculated values for the $\bar{\phi}_g$ may be used in the procedure. Equations (34) is in the same form (32) as equations (28) and (31), however, rather than solve the complete set of equations to obtain a new total scalar flux vector,

$$\bar{\phi}^k = \left[\phi_1^k, \phi_2^k \cdots \phi_G^k\right]$$

each component of the vector may be substituted into the calculation as soon as it is available. Thus, while ϕ^k is being determined, the latest ϕ^k values may be operated on by the diagonal and lower triangular matrices while the upper triangular matrix must use the previous values, ϕ^{k-1}. This scheme will be retained in all the quadrature variations subsequently introduced.

Before proceeding, an algorithm due to L. Cesari [18] will be introduced. Assume that the true solution to the transport equation, taken to have the form of equation (32),

$$\bar{\phi} = |m|\bar{\phi} + \bar{m}_1 \tag{32a}$$

may be approximated by finding the solution to a similar problem based on a less complex matrix, $|n|$.

$$\bar{\phi}_1 = |n|(\bar{\phi}_1 + \bar{m}_1) \tag{32b}$$

which has the solution

$$\bar{\phi}_1 = \left(|\vartheta| - |n|\right)^{-1} |n|\bar{m}_1 \tag{32c}$$

Let the true solution be the sum of two terms

$$\bar{\phi} = \bar{\phi}_1 + \bar{m}_1 \tag{32d}$$

then substituting (32d) into (32a)

$$\bar{\phi} = \bar{\phi}_1 + \bar{m}_1 = |m|\bar{\phi}_1 + |m|\bar{m}_1 + \bar{m}_1 \tag{32e}$$

and, to put both (32a) and (32b) into the same form, this becomes

$$\bar{\phi}_1 = |m|\left(\bar{\phi}_1 + \bar{m}_1\right) \tag{32f}$$

Now let the true solution, $\bar{\phi}$, be approximated by a series of terms

$$\bar{\phi} = \bar{\phi}_1 + \bar{m}_1 + \bar{\phi}_2 \tag{32g}$$

in which the solution consists of (32d) and a residue term, $\bar{\phi}_2$, involving the difference between the true solution and the approximate result. Substituting (32g) back into (32a),

$$\bar{\phi} = |m|\bar{\phi} + \bar{m}_1 = |m|\bar{\phi}_1 + |m|\bar{m}_1 + |m|\bar{\phi}_2 + \bar{m}_1 \tag{32h}$$

$$\bar{\phi}_2 = |m|\,\bar{\phi}_1 + \bar{m}_1 + |m|\bar{\phi}_2 - \bar{\phi}_1$$

which is of the same form as the original (32a)

$$\bar{\phi}_2 = |m|\bar{\phi}_2 + \bar{m}_2 \tag{32i}$$

if the modified term, $\bar{m}_2$, is given by

$$\bar{m}_2 = |m|\left(\bar{\phi}_1 + \bar{m}_1\right) - \bar{\phi}_1 \tag{32j}$$

Putting (32b) into (32j) returns, for $\bar{m}_2$,

$$\bar{m}_2 = |m|\left(\bar{\phi}_1 + \bar{m}_1\right) - |n|\left(\phi_1 + \bar{m}_1\right) \tag{32k}$$

or

$$\bar{m}_2 = \left(|m| - |n|\right)\left(\bar{\phi}_1 + \bar{m}_1\right) \tag{32l}$$

thus, as the matrix $|n|$ approaches $|m|$, the term $\bar{m}_2$ will approach zero. As is evident from equation (32c), the value of the residue term, $\bar{\phi}_2$, found from (32i) will also approach zero. The accuracy of the approximate solution, (32g), is then good if $|n| \to |m|$.

This same procedure may be repeatedly applied in order to obtain a series form of solution for $\bar{\phi}$:

$$\bar{\phi} = \sum_{n=1}^{N-1} (\bar{\phi}_n + \bar{m}_n) + \bar{\phi}_N \qquad (32m)$$

such that

$$\bar{\phi}_n = |\eta|\left(\bar{\phi}_n + \bar{m}_n\right)$$

and

$$\bar{m}_n = \left(|\mathcal{M}| - |\eta|\right)\left(\bar{\phi}_{n-1} + \bar{m}_{n-1}\right)$$

This algorithm has been applied by Kopp [19][20] to the transport equation to obtain the Synthetic Method. In this method repeated use of the $|\eta|$ matrix is made to calculate the terms of the series solution to the problem. The major difficulty in applying the method is in selecting an $|\eta|$ matrix which is a good approximation to $|\mathcal{M}|$ but is more readily solvable. The calculation of the terms $\bar{m}_n$ may also be difficult since they require use of the matrix $|\mathcal{M}| - |\eta|$ which may be more complicated than the original $|\mathcal{M}|$. The method has been applied by Crawford and Friedman [21] and Gelbard and Hageman [22] using the three term series (32g). In these applications the approximation made is that the $|\eta|$ matrix is defined by either the diffusion equation or an S_2 quadrature and the $|\mathcal{M}|$ matrix by a high order (S_6) discrete ordinates calculation or by a Monte Carlo calculation of the transport equation. Since neither of these $|\eta|$ matrix approximations to the $|\mathcal{M}|$ matrix satisfies closely the condition that $|\eta| \to |\mathcal{M}|$ the residual term, $\bar{m}_2$, may be large and the solution in error.

The Ray Effect

The S_n method, since its inception, has been used successfully on a great variety of problems. It had generally been assumed that even a relatively low order S_n approximation would yield scalar flux distributions sufficiently accurate for most problems. The quadrature orders most often used were either S_2 or S_4. More recently, however, it has been found that anomalous effects [23] leading to quite incorrect flux distributions could be present even in seemingly simple configurations. The phenomenon has been shown to be due to the nature of the discrete ordinates approximation to the angular integral in the transport equation [24]. If the analytic integral over the unit sphere defined by $\hat{\Omega}$

$$\phi(r)=\int_{\hat{\Omega}} \psi(\overline{r},\hat{\Omega})d\hat{\Omega}$$

is replaced by the discrete ordinates summation

$$\phi(r) = \sum_{m=1}^{M} w_m \underline{\psi}_m(\overline{r}) \qquad (10)$$

over a limited number of characteristic directions, then the accuracy of the substitution depends strongly on the degree to which the central average angular flux, $\underline{\psi}_m$, corresponds to the true average value of the angular flux on each portion, $\Delta\Omega_m$, of the unit sphere. For example, figure 4 shows a two dimensional representation of a possible angular flux distribution. It is evident that any placement of a small number of characteristic directions, such as that indicated by the $\underline{\psi}(\Omega_m)$ in

1. Average angular flux calculated for quadrant is along direction $\hat{\Omega}_m$.

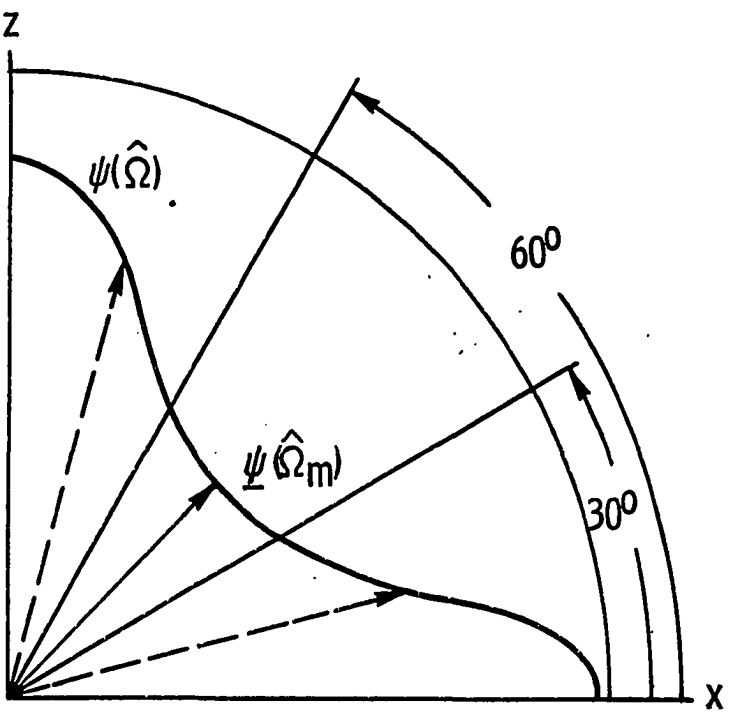

Figure 4. - Angular flux distribution - S_2 calculation (2D), [solid line].

the figure, is unlikely to yield a valid average for use in equation (10). Again, from the same figure, is it possible for the average value along a particular characteristic direction to be either overestimated or underestimated. The results of reference [23] furnish a good example of the overprediction of the angular fluxes while [24] demonstrates an extreme case of underprediction. In either case, the resulting scalar fluxes are in error, the subsequent source calculation not valid, and the final solution incorrect. Since the particles in a discrete ordinates approximation may be considered to be transmitted along characteristic directions, or "rays", such instances of incorrect averaging and their propagation are referred to as examples of the "ray effect". This situation is further complicated by the fact that existence of the ray effect in a particular case may not be obvious and all S_n solutions are, therefore, suspect.

The angular quadratures presently used in discrete ordinates calculations are also subject to restrictions which tend to aggravate this incorrect averaging. The following brief discussion outlines the salient features concerning the generation of angular quadrature sets, [11] and [13], which are valid in any number of spatial dimensions:

The characteristic directions define a number of points on the unit sphere. Each point may be described by its direction cosines (μ, η, ξ) with respect to the x, y and z axes. There are several ways in which weighting factors may be assigned to each direction. Since these are somewhat arbitrary the quadrature sets used will generally utilize weights proportional to the area of the unit sphere represented by each point. The convention of stating the weighting factors in units

of 4π, to match the analytic integral, will be adhered to so that one condition on these is

$$\sum_{m=1}^{M} w_m = 1.0 \tag{35}$$

Since there is no way of determining in advance the characteristic directions best suited for each problem, the standard requirement that the solution be invariant with respect to rotation of the coordinate system is introduced. That is, the solution must not depend on the orientation of the configuration with respect to the coordinate system. The replacement of the continuum of directions in the analytic integral by a finite number of characteristic directions precludes rotational-reflection invariance with respect to arbitrary rotations but allows the substitution of invariance with respect to 90° rotations and to reflections about any axis. Consideration of the quadrature set in figure 2 indicates that this invariance is possible only if the points on each octant are identical. Thus, μ must map into η or ξ, as indicated, and the direction cosines must be permutations of one set of values. Furthermore, if the solution is to be invariant, the weights assigned to each point must correspond to those of the equivalent point in all other octants. It is sufficient, then, to consider only one octant in the derivation of formulae for generating the characteristic directions.

If the points on each octant of the unit sphere are arranged in $n/2$ levels, the total number of points,

$$n(n + 2) \tag{35}$$

is taken to define an S_n approximation of order $n(n = 2,4,6, \ldots)$. It has been shown that the law of direction cosines in conjunction with the condition of rotation-reflection invariance determines a formula for the values of the $n/2$ levels on the unit sphere [11]

$$\mu_i^2 = \mu_1^2 + (i - 1)\left[\frac{2}{i - 2}(1 - 3\mu_1^2)\right] \qquad i=1,\ldots\frac{N}{2} \tag{36}$$

where μ_1 is the smallest value. One immediate consequence of rotation-reflection invariance is a severe limitation on the arrangement of points on the unit sphere. Thus, regardless of the order of the quadrature, there is only one independent value for the direction cosines. Every characteristic direction is fixed, even though the points may not be well distributed, once μ_1 is chosen. In addition, use of the formulae of [11] to generate invariant angular quadrature sets of order greater than S_{22} has not been possible due to the appearance of negative weights which disrupt the calculation. The use of an arbitrarily large number of characteristic directions to correct ray effects is, therefore, precluded.

It is evident that the existence of ray effects is due to use of a limited number of characteristic directions. The anomalous results obtained are compounded by limitations on the original placement of these directions and the retention of a single fixed angular quadrature set for each calculation. Some suggestions have been made for minimizing the magnitude of the ray effect by altering the treatment of the characteristic directions. Thus, Kaplan [25] has proposed a space-angle synthesis approach in which the quadrature directions are permitted to vary as a function of the spatial coordinates. This is done

to interrupt particle transmission along the fixed characteristic directions and so achieve better average angular fluxes. Another approach has been formulated by Brissenden [26] and involves using the neutron balance in each mesh interval to choose optimum values for the characteristic directions. Each of these proposals involves appreciable alterations in the standard discrete ordinates application and, if implemented, offers no assurance of eventual convergence on the solution.

Angular Quadrature Decoupling

In this section, an alternative proposal for reduction of the ray effect will be presented. The basic feature of the approach is a method for varying the angular quadrature within the framework of the standard S_n application. Since the ray effect is geometric in nature, it is sufficient to consider equation (22), for the central average angular flux, as applied to the monoenergetic case. While the ray effect may be present in any multidimensional coordinate system, it is most evident in two dimensional (x,z) rectangular coordinates. For this case, equation (22) reduces to

$$\underline{\psi} = \frac{\mu\left(A_{i+1} + A_i\right)\psi_i + \xi\left(C_{k+1} + C_k\right)\psi_k + SV}{2\mu A_{i+1} + 2\xi C_{k+1} + \sigma^t V} \tag{37}$$

The use of equation (37) considerably simplifies the matrix $|a|$ of equation (28). For the monoenergetic case, the $|\delta|$ matrix of equation (25) reduces to one row while the summation of equation (10) is unchanged. As described in the Machine Solutions section, the angular fluxes will be calculated in the inner iterations with scalar sources being redetermined in each outer iteration.

The individual terms in the $|a|$ matrix may be associated with equivalent terms in the transport equation. Those terms containing μ and ξ relate to particle transport (uninterrupted transfer along the characteristic directions) while the scalar source term, SV, includes particle reorientation due to scattering collisions with the medium. Conventional application of the discrete ordinates requires that a complete inner iteration over all directions represented by the matrix $|a|$ be executed before the scalar fluxes may be used to update the source terms. An incorrect estimate of the particle transport may, however, be caused not only by the initial choice of quadrature directions but by the coupling between these directions. Consider the behaviour of equation (28) in a source free medium which is a perfect absorber. Then all the source terms, SV, are zero and particles can be present in the medium only if transmitted along the characteristic directions. If scattering is introduced, particles may be present due to angular reorientation caused by the scattering. Any process in which the angular orientation of the particles is altered tends to reduce the ray effect by disrupting transmission along the characteristic directions. According to equation (37), all terms involving these processes, both scattering and fission, are functions only of the scalar flux. In the standard S_n procedure, however, the coupling between directions, caused by determining all the angular fluxes prior to calculation of the scalar flux, may mask the effect of the angular redistribution terms. That is, in solving the matrix $|a|$ for a given spatial mesh interval, the individual components of some of the source terms

$$w_{m'm} \psi_{m'} \sigma^{s}_{g' \to g}$$

may be negligible when compared to the total source term

$$\sigma^{s}_{g\to g}\phi_{g} = \int \sigma^{s}(r,\hat{\Omega}' \to \hat{\Omega})\ \psi(r,\hat{\Omega}')d\hat{\Omega}'$$

inferred by the integral.

In order to illustrate this postulate, a configuration similar to that used in reference [24] to discuss ray effects will be introduced. It is, as shown in figure 5, a rectangle having a source region at one end. For the present, the discussion is confined to fixed (constant) source problems with scattering but no fission. Since it is not possible to obtain analytical solutions to problems of this type, some special [13] high order quadrature sets, S_{32} and S_{16}, which are valid only in two dimensional configurations, will be taken to return reasonably correct results. As a first test case, let the source free portion of the medium have a scattering ratio, $c = \sigma^{s}/\sigma^{t}$, of one-half and a total cross-section of one. Assume that the solution may be obtained by application of a standard invariant S_6 quadrature. The matrix $|a|$ in the form of equation (37), is then solved for all $\frac{6}{2}(6+2) = 24$ directions and $12 \times 5 = 60$ mesh intervals and the complete set of ψ_m found and summed according to equation (10). The scalar flux distribution for the edge and end (the problem is symmetrical about the x axis) of the test configuration is shown in table 1. The results are seen to be poor, particularly at the far end of the rectangle where the ray effect causes a concave, rather than convex, flux shape. To test the postulate made, the same S_6 quadrature set is applied with, however, the matrix $|a|$ solved separately for each characteristic

1. Spatial mesh as shown. All intervals 1x1 centimeter.
2. Cross hatching denotes source region, (fixed or fission).
3. Interval numbering corresponds to tables 1, 2, 3, and 4.

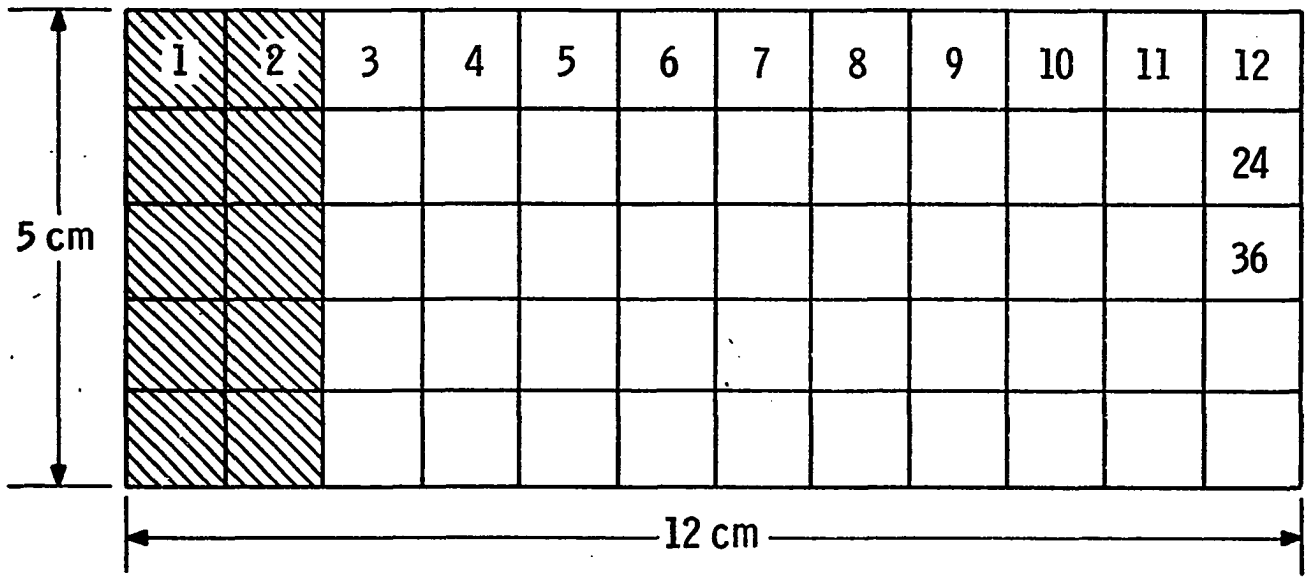

Figure 5. - Ray effect test case geometry.

TABLE 1

SCALAR FLUX DISTRIBUTION IN STANDARD AND FULLY DECOUPLED S_6 QUADRATURES

Interval number[a]	1	2	3	4	5	6	7
[b] S_6	0.771×10^{0}	0.679×10^{0}	0.256×10^{0}	0.656×10^{-1}	0.189×10^{-1}	0.591×10^{-2}	0.189×10^{-2}
[c] S_6	0.754×10^{0}	0.662×10^{0}	0.248×10^{0}	0.664×10^{-1}	0.199×10^{-1}	0.682×10^{-2}	0.252×10^{-2}
Interval number[a]	8	9	10	11	12	24	36
[b] S_6	0.613×10^{-3}	0.199×10^{-3}	0.666×10^{-4}	0.199×10^{-4}	0.659×10^{-5}	0.763×10^{-5}	0.750×10^{-5}
[c] S_6	0.987×10^{-3}	0.393×10^{-3}	0.157×10^{-3}	0.622×10^{-3}	0.238×10^{-4}	0.337×10^{-4}	0.369×10^{-4}

[a] Twelve edge and five end intervals of 1 cm, problem is symmetric about x direction.

[b] Calculated in standard method.

[c] Each direction calculated separately.

direction. In other words, a quasi-scalar flux, ϕ_m, is found for each direction $(\pm\mu,\pm\xi)$ by assuming that the weighting factors, w_s, for each separated set meet the condition of equation (35). These quasi, or decoupled, fluxes are then recombined according to the original point weights

$$\phi(r) = \sum_{m=1}^{M} \frac{w_m \phi_m}{w_s} \tag{38}$$

to obtain the revised solution.

The results of these calculations are shown in table 1 which indicates that particle transmission to the far end of the configuration is greatly increased by decoupling the matrix $|a|$. It is obvious that complete decoupling of the angular flux matrix is not desirable since it allows overemphasis of one particular direction and increases the time required to obtain the final solution by requiring an outer iteration for each direction. However, due to the nature of the derivation of standard quadrature sets, it is always possible to separate them, according to the different weighting factors, so as to obtain subsets which have the same number of points as those in some lower order set. The S_6 set of figure 6 is an example. The two possible weighting factors are indicated and if the set is so decoupled, two subsets of three points (in each octant) are obtained. It is also possible to apply this technique by replacing the higher order set with multiple lower order sets having an equivalent number of characteristic directions. This approach allows more lattitude in the placement of points since an independent value for μ_1 may be specified for each lower

1. Arrangement of point weights is as shown.
2. Decoupling is by original point weights. Solid and open circles indicate resulting two sets of three points each.

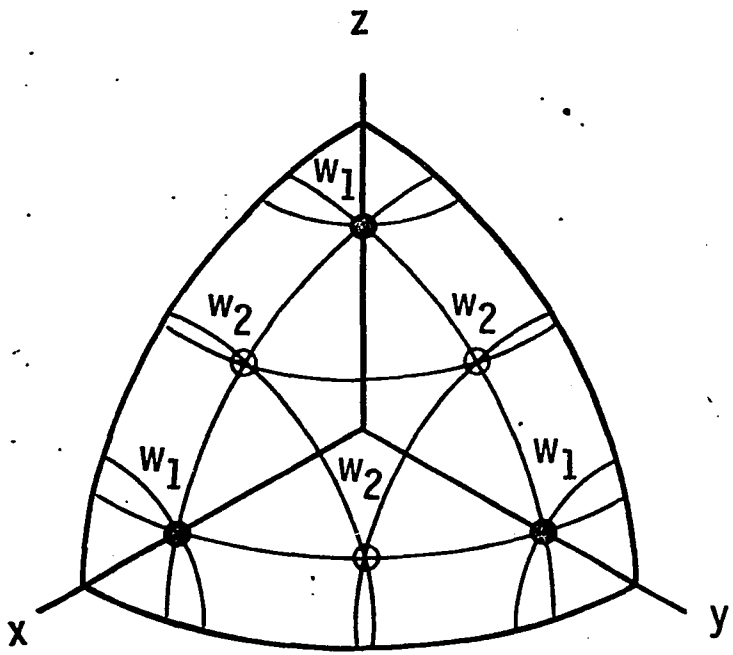

S_6 Direction cosines and weights	
μ	w
0.9305	0.0458
.6831	.0375
.2582	

Figure 6. - Decoupling of standard S_6 quadrature set.

order set. Both the decoupling and multiple lower order approaches are now applied to the test problem. The scalar flux is found by replacing the S_6 $|a|$ matrix with two subset matrices. One is the decoupled S_6 set while the other consists of two independent S_4 quadrature sets, shown in figure 7, with differing values of μ_1^2. The edge and end scalar flux distributions for these calculations are given in table 2 along with the standard S_6 result and the high order S_{32} solution. While the orders of magnitude variation in the flux distribution precludes general graphical presentation, figure 8 exhibits the end fluxes for these cases. As seen before, the straight S_6 solution is extremely poor, particularly at the far end of the configuration where it is low in magnitude and concave rather than convex. The two independent S_4 sets although low in magnitude, return the correct end flux shape. The decoupled $2S_4(S_6)$ sets demonstrate a significant improvement when compared with the standard application. Not only are the magnitudes substantially correct but the fluxes are extremely close to those of the S_{32} solution. Since it is not possible to compare the independent subsets with any base calculation, the process of decoupling the matrix according to the point weights is applied to some additional higher order quadratures. In table 3 are presented the results of separating an S_8 quadrature into three ($1S_2$, $1S_4$, and $1S_6$) subsets and an S_{12} quadrature into five ($3S_4$ and $2S_6$) subsets. Pertinent details of each of these invariant angular quadrature sets are given in figures 9 and 10. Comparison of these results with those of the standard application for each set show considerable improvement for the decoupled S_8 set. Neither the original S_{12} set, nor the

1. Use of two independent (S_4) sets to replace one (S_6) higher order set.
2. As shown by dashed lines, additional free parameters (μ_m) are created.

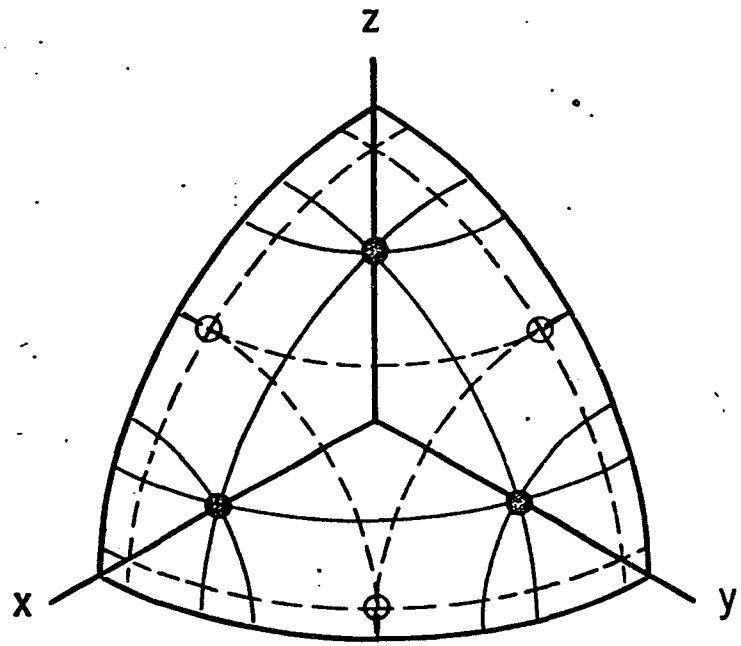

$2S_4$ Direction cosines and weights	
μ	w
● Set 1	
0.8819 .3333	0.0833
○ Set 2	
0.7041 .0918	0.0833

Figure 7. - Independent S_4 sets to replace standard S_6 set.

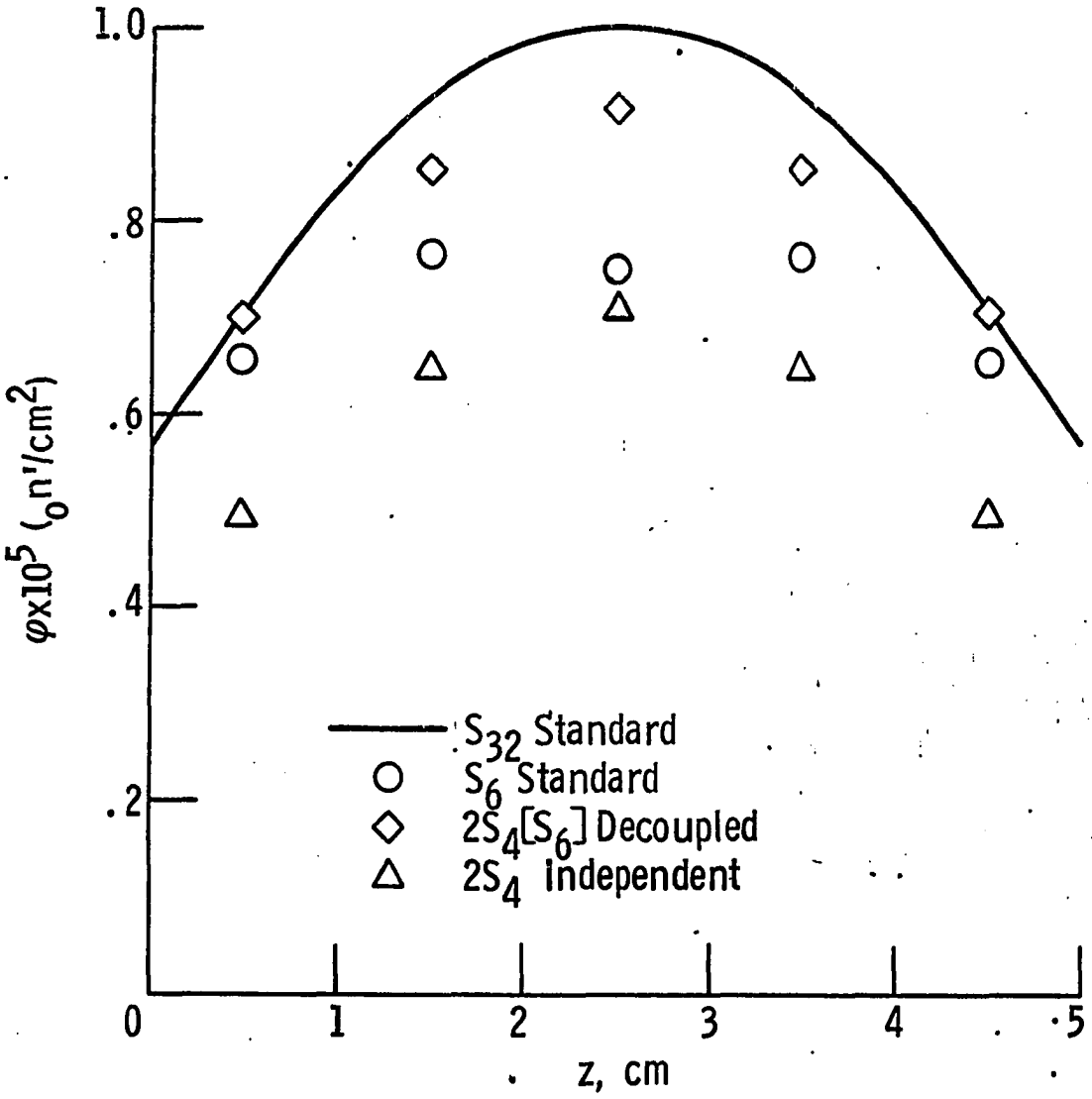

Figure 8. - Standard test configuration ($\sigma^a = \sigma^s = 0.5$) end scalar flux distribution.

TABLE 2

SCALAR FLUX DISTRIBUTION IN ($\sigma^a = \sigma^s = 0.5$) TEST CASE

Interval number	1	2	3	4	5	6	7
[a] S_{32}	0.810×10^{0}	0.714×10^{0}	0.254×10^{0}	0.632×10^{-1}	0.191×10^{-1}	0.593×10^{-2}	0.189×10^{-2}
[a] S_6	0.771×10^{0}	0.679×10^{0}	0.256×10^{0}	0.656×10^{-1}	0.189×10^{-1}	0.591×10^{-2}	0.189×10^{-2}
[b] S_6	0.771×10^{0}	0.679×10^{0}	0.256×10^{0}	0.659×10^{-1}	0.189×10^{-1}	0.587×10^{-2}	0.187×10^{-2}
[c] $2S_4 \rightarrow S_6$	0.812×10^{0}	0.728×10^{0}	0.291×10^{0}	0.762×10^{-1}	0.214×10^{-1}	0.646×10^{-2}	0.194×10^{-2}
Interval number	8	9	10	11	12	24	36
[a] S_{32}	0.595×10^{-3}	0.204×10^{-3}	0.670×10^{-4}	0.221×10^{-4}	0.710×10^{-4}	0.932×10^{-5}	0.101×10^{-4}
[a] S_6	0.613×10^{-3}	0.199×10^{-3}	0.666×10^{-4}	0.199×10^{-4}	0.659×10^{-5}	0.763×10^{-5}	0.750×10^{-5}
[b] S_6	0.625×10^{-3}	0.213×10^{-3}	0.694×10^{-4}	0.238×10^{-4}	0.701×10^{-5}	0.859×10^{-5}	0.919×10^{-5}
[c] $2S_4 \rightarrow S_6$	0.554×10^{-3}	0.169×10^{-3}	0.515×10^{-4}	0.162×10^{-4}	0.485×10^{-5}	0.643×10^{-5}	0.716×10^{-5}

[a] Calculated in standard method.

[b] Calculated using decoupled S_n subsets.

[c] Calculated using two S_4 subsets to replace S_6 set.

TABLE 3

SCALAR FLUX DISTRIBUTION IN ($\sigma^a = \sigma^s = 0.5$) DECOUPLED HIGHER ORDERS

Interval number	1	2	3	4	5	6	7
$^aS_{32}$	0.810×10^{0}	0.714×10^{0}	0.254×10^{0}	0.632×10^{-1}	0.191×10^{-1}	0.593×10^{-2}	0.189×10^{-2}
$^aS_{8}$	0.780×10^{0}	0.687×10^{0}	0.256×10^{0}	0.597×10^{-1}	0.168×10^{-1}	0.499×10^{-2}	0.158×10^{-2}
$^bS_{8}$	0.779×10^{0}	0.687×10^{0}	0.263×10^{0}	0.601×10^{-1}	0.167×10^{-1}	0.494×10^{-2}	0.159×10^{-2}
$^aS_{12}$	0.789×10^{0}	0.695×10^{0}	0.253×10^{0}	0.694×10^{-1}	0.211×10^{-1}	0.672×10^{-2}	0.218×10^{-2}
$^bS_{12}$	0.788×10^{0}	0.694×10^{0}	0.253×10^{0}	0.694×10^{-1}	0.209×10^{-1}	0.659×10^{-2}	0.216×10^{-2}
Interval number	8	9	10	11	12	24	36
$^aS_{32}$	0.595×10^{-3}	0.204×10^{-3}	0.670×10^{-4}	0.221×10^{-4}	0.710×10^{-4}	0.932×10^{-5}	0.101×10^{-4}
$^aS_{8}$	0.518×10^{-3}	0.188×10^{-3}	0.646×10^{-4}	0.200×10^{-4}	0.622×10^{-5}	0.702×10^{-5}	0.714×10^{-5}
$^bS_{8}$	0.566×10^{-3}	0.189×10^{-3}	0.667×10^{-4}	0.225×10^{-4}	0.727×10^{-5}	0.870×10^{-5}	0.890×10^{-5}
$^aS_{12}$	0.723×10^{-3}	0.263×10^{-3}	0.896×10^{-4}	0.298×10^{-4}	0.985×10^{-5}	0.127×10^{-4}	0.135×10^{-4}
$^bS_{12}$	0.735×10^{-3}	0.261×10^{-3}	0.903×10^{-4}	0.324×10^{-4}	0.109×10^{-4}	0.142×10^{-4}	0.151×10^{-4}

[a]Calculated in standard method.

[b]Calculated using decoupled S_n subsets.

1. Decoupling by point weights yields one S_2 (1 point), one S_4 (3 points), and one S_6 (6 points) set.

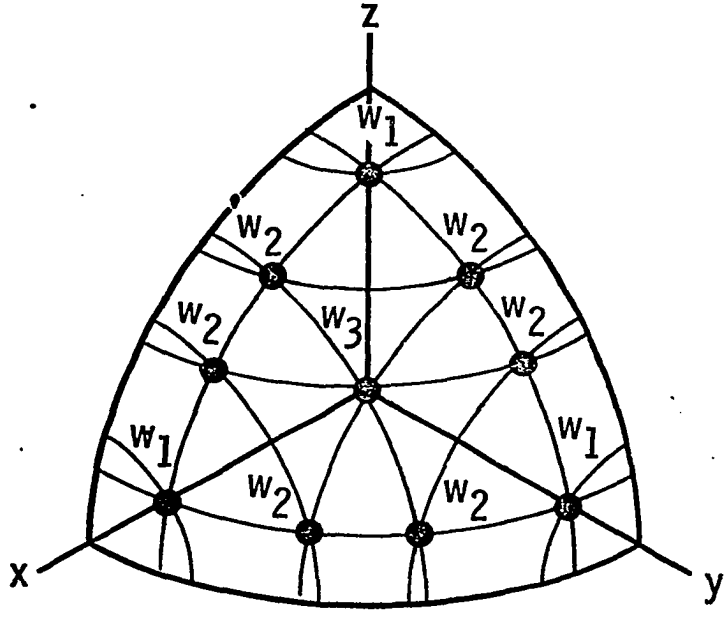

S_8 Direction cosines and weights	
μ	w
0.9512	0.0635
.7868	.0457
.5773	.0354
.2182	

Figure 9. - Decoupling of standard S_8 quadrature set.

1. Decoupling by point weights yields three S_4 (3 points), and two S_6 (6 points) sets.

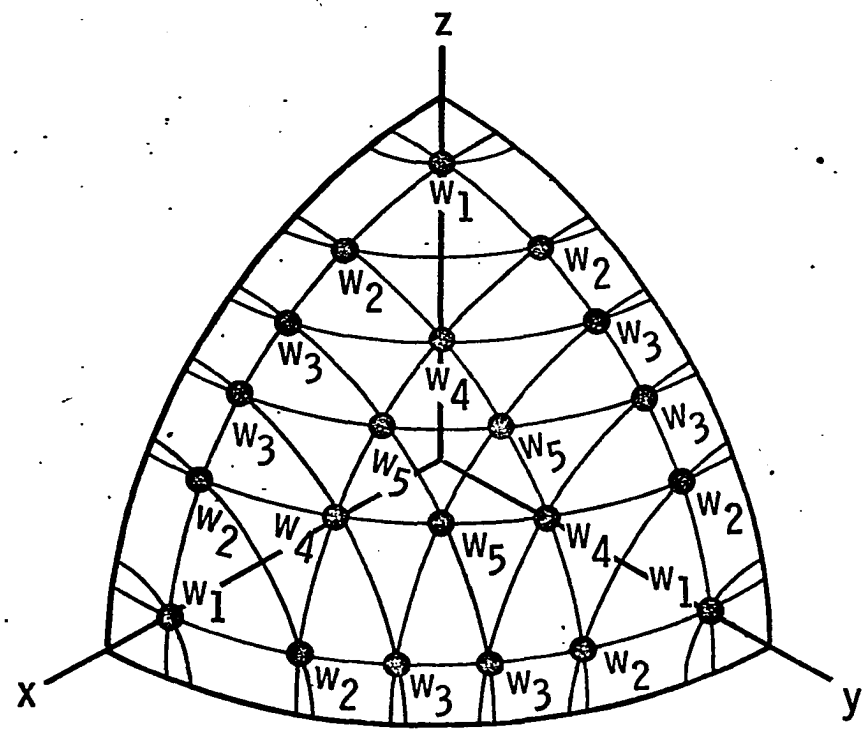

S_{12} Direction cosines and weights	
μ	w
0.9716	0.0177
.8723	.0140
.7600	.0093
.6280	.0126
.4595	.0065
.1672	

Figure 10. - Decoupling of standard S_{12} quadrature set.

decoupled S_{12}, yield particularly accurate solutions. This may be attributed to the fact that the characteristic directions in this set are not initially well chosen.

The major limitation on any use of multiple subsets to replace a standard quadrature set is the magnitude of the scattering cross section in the medium under consideration. In a pure absorber, the source term, SV, vanishes and the angular fluxes calculated are identical for each direction whether the matrix is decoupled or not. No improvement is, therefore, expected in the scalar flux distribution. Since the major effect of replacing the $|A|$ matrix with submatrices is to augment particle reorientation, less improvement may be anticipated with diminished scattering. To demonstrate this, the base S_{32} and the S_6 problems described above are recalculated with both the absorption and scattering cross sections reduced by a factor of ten. The resulting scalar flux distributions are shown in table 4 and the end fluxes in figure 11. As expected, only minor improvement is noted in the decoupled subsets. The two independent subsets, although returning fluxes whose magnitude seems too high, do preserve the correct flux shape. It should be noted that problems of this type (i.e., with little scattering and no sources) represent an extreme test of the discrete ordinates approximation. Even the S_{32} base calculation of this test case, also given in table 4, demonstrates points of inflection in the end flux distribution which are not physically realistic.

For the next test case, the fixed source is replaced with a fission source which is, of course, dependent on the scalar flux. This test case now represents an eigenvalue problem and requires several

TABLE 4

SCALAR FLUX DISTRIBUTION IN ($\sigma^s = \sigma^a = 0.05$) TEST CASE

Internal number	1	2	3	4	5	6	7	8	9	10	11	12	24	36
[a] S_{32}	0.811	0.708	0.421	0.266	0.187	0.139	0.103	0.0785	0.0617	0.0485	0.0386	0.0305	0.0323	0.0354
[a] S_6	0.774	0.672	0.441	0.275	0.174	0.122	0.101	0.0808	0.0669	0.0555	0.0419	0.0312	0.0179	0.0122
[b] S_6	0.774	0.672	0.442	0.275	0.174	0.122	0.101	0.0809	0.0669	0.0546	0.0421	0.0313	0.0180	0.0124
[c] $2S_4 \rightarrow S_6$	0.814	0.716	0.462	0.297	0.213	0.149	0.109	0.0864	0.0703	0.0556	0.0441	0.0349	0.0421	0.0471

[a] Calculated in standard method.

[b] Calculated using decoupled S_6 subsets.

[c] Calculated using two S_4 subsets to replace S_6 set.

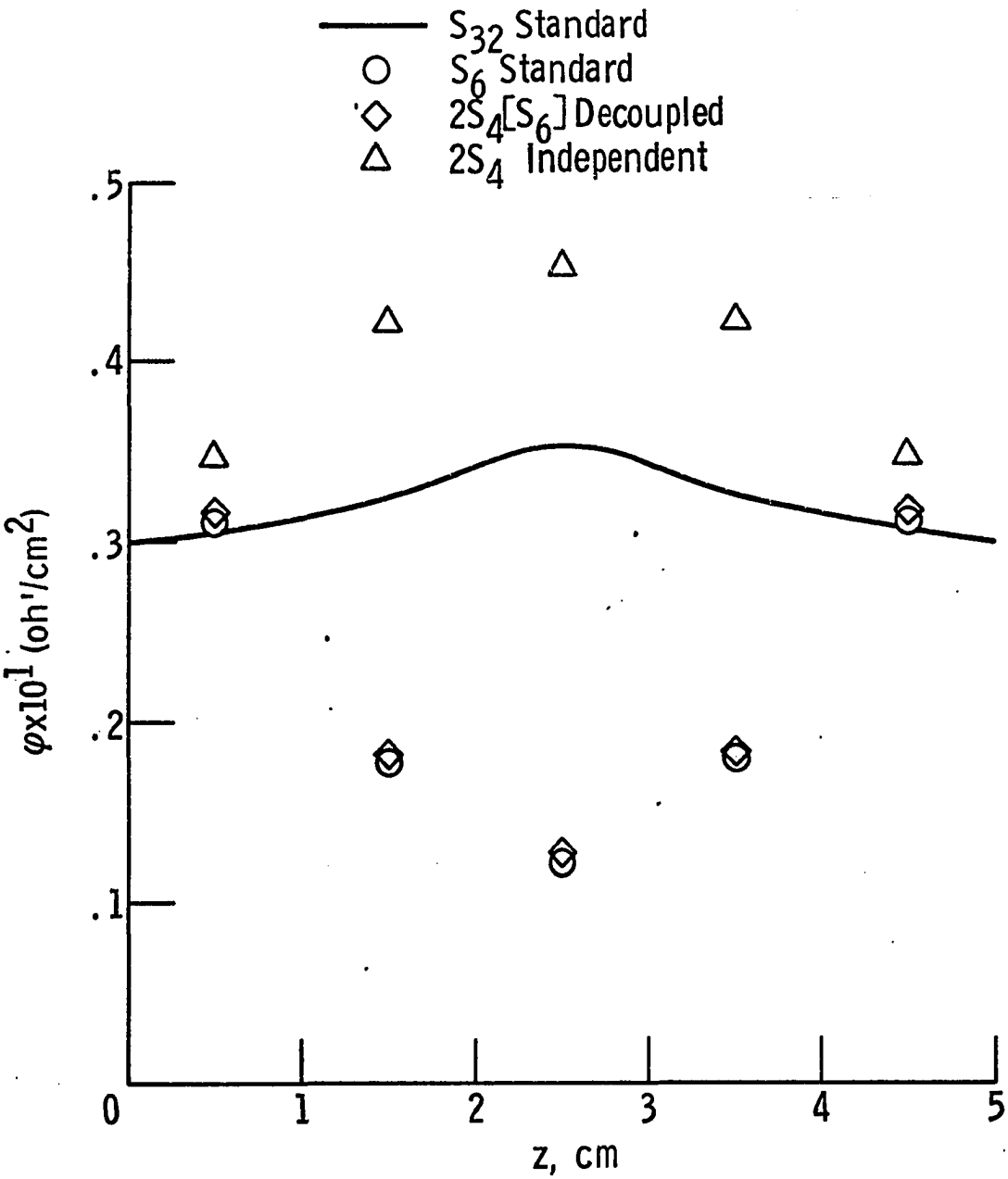

Figure 11. - Standard test configuration ($\sigma^a = \sigma^s = 0.05$) end scalar flux distribution.

inner and outer iterations to converge. This allows an alternative procedure in the method being described to be attempted. Since more than one outer iteration, in which the terms dependent on the scalar fluxes are recalculated, is necessary, the decoupled quadrature sets may be used separately in the inner (or $|a|$ matrix angular flux calculation) and the resultant scalar fluxes combined in each outer (or $|\ell|$ matrix) iteration. This procedure is of interest since it has a common basis with the proposals of references [25] and [26]. The alternation of the quadrature sets is roughly equivalent to rotating points on the unit sphere in order to disrupt the particle transmission. As all the quadrature sets used in implementing this version behaved similarly, only the S_6 test results, along with the S_{32} control distribution, are reported. The permutations run included the standard S_6 invariant set, the decoupled S_6 set with full convergence on each subset prior to flux recombination, and the "rotating" decoupled S_6 set using a varying number of inner iterations on each subset. In order to exhibit the results graphically, the flux distributions at the end of the test configuration are shown in figure 12. The S_{32} results are expected to be substantially correct for this case. As is evident, the "rotating" decoupled sets yield a flux distribution which is better than that of the standard S_6 application. They do not, however, even with the fission source, show as much improvement as the decoupled sets in which full convergence is attained prior to recombining the scalar fluxes as in equation (38). They are also more slowly convergent and, therefore, the original method proposed must be judged somewhat superior.

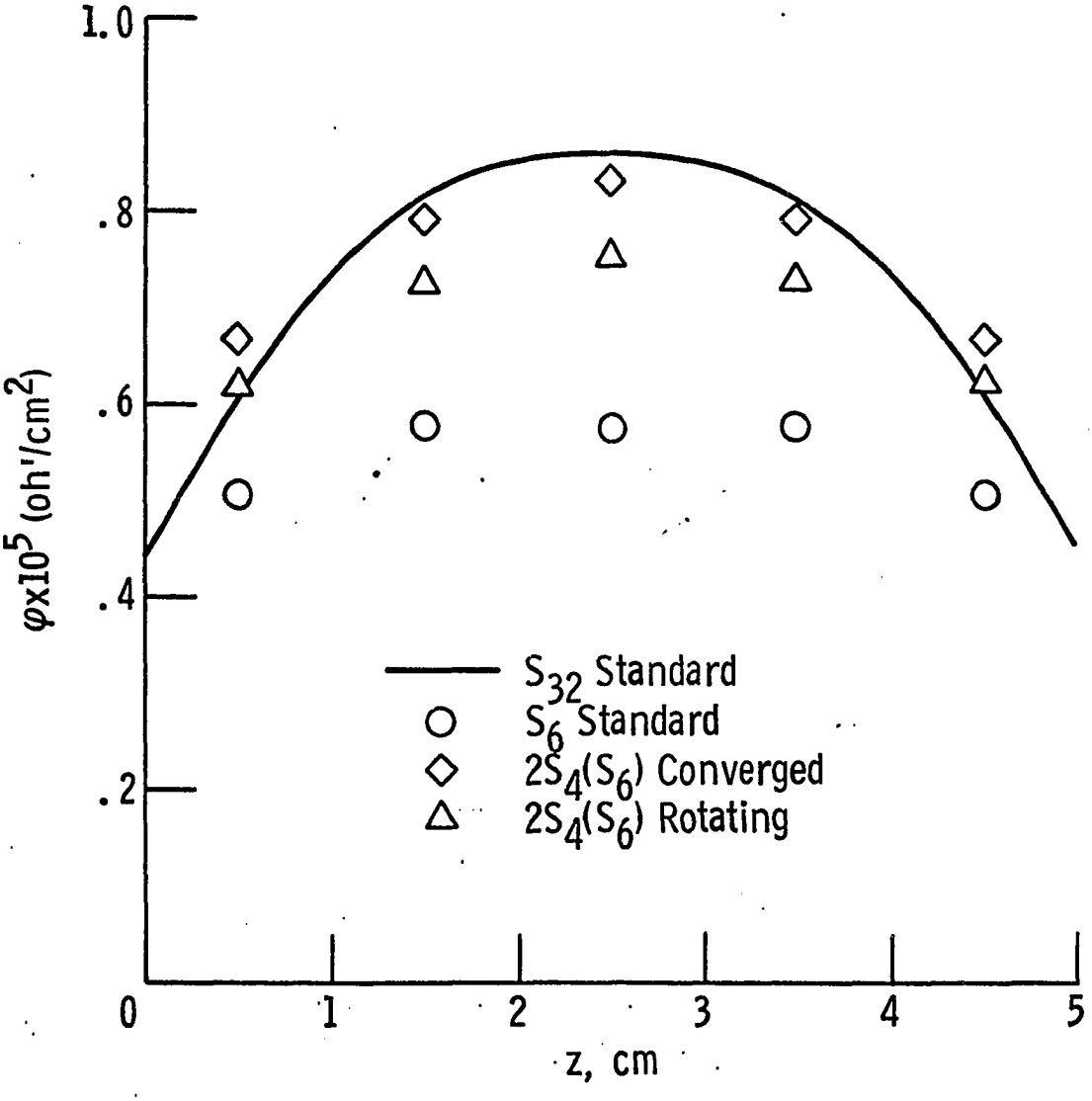

Figure 12. - Standard test configuration (fission source) end scalar flux distribution.

Ray Effect Conclusions

The method developed in the preceding sections has been shown to be effective in reducing the magnitude of the ray effect in certain classes of problem. It is of interest, at this point, to summarize the causes of this effect and to briefly review other suggested methods of eliminating it.

The ray effect is caused by the necessity for evaluating the angular integral in the transport equation by numerical methods. As exemplified by figure 4, the use of a small number of ordinates, N, in the substitution of equation (9)

$$\int_{-1}^{1} \psi(\vec{r},\hat{\Omega}) = \sum_{n=1}^{N} w_n \psi_n(\vec{r},\Omega_n) \tag{9}$$

cannot be expected to yield valid results where the angular flux distribution varies rapidly. Again in figure 4, the magnitude of the calculated angular flux in each thirty degree segment will be that at the point where the discrete direction intercepts the distribution, $\psi(\vec{r},\hat{\Omega})$, and not, in general, equal to the correct average over the angular interval. The resultant effect of such incorrect averaging manifests itself primarily in two ways. First, the characteristic directions may not intercept source regions at the points necessary to obtain a valid average source. Second, the calculation of particle transmission along the characteristic directions may be incorrect due to the coupling between directions. However, since any numerical evaluation of the integral requires the use of a finite number of discrete ordinates, alternative methods for minimizing the ray effect

must depend, as does the present method, on increasing the efficiency of the angular quadrature used.

In the method suggested by Kaplan [25], the underlying concept is that of extending synthesis type approximations [27] to the space-angle quadratures required by the transport equation. In space-angle synthesis the flux distribution is found as a linear combination of a specified set of "trial functions". These trial functions are actually angular flux estimates which are permitted to vary with position in the spatial mesh. This approach has been implemented [28] by using such discontinuous trial functions to solve some Milne type problems. An extension of the method to apply a low order space-angle synthesis approximation to some more practical monoenergetic, fixed source problems has also been accomplished [29]. While the method is still under development, its utility is limited for several reasons: the accuracy of the solution depends strongly on the degree to which the trial functions approximate the true solution. Obtaining such functions is, to a large degree, equivalent to obtaining solutions to the transport equation. While a given set of trial functions may be used for problems having similar configurations, new trial functions must be obtained for arbitrary configurations. In addition, the solutions admit of discontinuities which may not be acceptable in many types of problem. For these reasons, use of the method seems restricted to repetitive application on problems having similar physical dimensions and flux distributions which also contain large, nearly homogeneous regions.

The proposed method of Brissenden [26] is more difficult to evaluate since it has not been implemented. The basic principle is that of calculating the particle balance in each spatial mesh interval. This balance is then to be used in optimizing the placement of the characteristic directions. While the extension of the approach to high angular order multidimensional geometries is not clearly understood, there are several aspects which would seem to mitigate against its use. One is that the major purpose of the discrete ordinates is to determine the angular distribution. That is, while the correct particle balance for each interval may improve the initial source calculation, it is essential that the correct proportion of particles transported in each direction be known. Optimization of the characteristic directions is difficult since it is only through the use of a given set of directions that the particle transmission through the orthogonal interval faces can be estimated. Nor would the "optimum" set of directions in one interval necessarily correspond to those of another interval. If more than one set of directions is used in the spatial mesh, the calculation of the particle balance across each face and its subsequent re-distribution along each new characteristic direction in the new set would be extremely time consuming and permit of a large number of discontinuities in the angular flux. Thus, any further evaluation must await application of the method to some practical problems.

The method presented in this paper relies on the use of a linear combination of solutions to lower order angular quadrature problems. The mixing coefficients are either the weighting factors (for the

multiple decoupled quadratures) or simple averages (for the multiple independent quadratures). The use of multiple lower order quadrature sets may be related to the causes of the ray effect discussed above. If the incorrect averaging is due to improper detection of the source, multiple sets allow more latitude in placement of the set directions and can improve the source calculation. If the incorrect particle transmission is due to coupling between directions in the set, some improvement may be expected when the set is decoupled since the transmission along the individual directions is enhanced. The degree of improvement in this approach is dependent on the physical composition of the medium. Thus, limits may be placed on the general method of substituting multiple sets for a single higher order set by considering the behaviour of equation (37)

$$\underline{\psi} = \frac{\mu(A_{i+1} + A_i)\psi_i + \xi(C_{k+1} + C_k)\psi_k + SV}{2\mu A_{i+1} + 2\xi C_{k+1} + \sigma^t V} \qquad (37)$$

under varying conditions. Since any scalar particle source tends to obscure ray effects, it is sufficient to consider equation (37) as applied to monoenergetic, fixed source problems. Under these conditions, the coefficient s_{gg} of equations (28) is equal to the self-scattering ($\sigma^s_{g\to g}$) cross-section and the source term, SV, becomes $\phi\sigma^s_{g\to g}V$. Then, consider equation (37) in a purely absorbing medium. There is no scattering and the angular fluxes do not depend on the scalar fluxes. The scalar fluxes calculated by summing as in equation (10) will be the same whether the quadrature set is decoupled or not.

Thus, in the limit of a pure absorber, the solution for the decoupled sets will be identical to that of the original quadrature set. In a purely scattering material it is more difficult to analytically establish a limit on the use of multiple sets. However, the magnitude of the source terms, SV, becomes so large that the scalar sources predominate. Under these conditions, the multiple sets again tend to approach the same solution as that returned by the original set. When the test configuration described in the previous section is solved for a pure scatterer, for example, the decoupled sets return the same results as the original quadratures. Thus, for well chosen quadrature subsets, the method yields results which tend to be bounded by the solutions of the single higher order set.

There are several other advantages to this approach. The rotationally invariant quadrature sets are limited to orders less than S_{22}, due to the appearance of negative weights. In the method presented, however, more characteristic directions may be employed by linearly combining the results of multiple high order calculations. In addition, the other proposed methods contain features which may disrupt the convergence properties of the discrete ordinates approximation. The present method, however, is applied within the framework of the approximation, and retains the convergence properties of the original procedure.

In summary, it does not seem that any numerical method, which must rely on a limited number of discrete ordinates, can completely

eliminate the ray effect. While significant improvement has been obtained in some problems by application of the method developed, the disparities noted in the high order results for the second test cases indicate that only the use of a larger number of angular intervals, either standard or multiple, can insure accurate results. Unfortunately, problems which require high order quadratures, either angular or spatial, are extremely time consuming due to the number of angular fluxes which must be determined for each spatial interval in each iteration. For example, in a two space dimension configuration requiring ten spatial intervals for each coordinate direction (a relatively small problem), there are 100 mesh intervals. If it is found necessary to use, say, an S_{32} calculation rather than an S_8, use of equation (35) shows that

$$S_8 = n(n + 2) = 80 \times 10^2 = 8000 \text{ directions}$$

$$S_{32} = n(n + 2) = 1088 \times 10^2 = 108{,}800 \text{ directions}$$

the number of directions increases radically. Since each inner iteration over the spatial mesh requires not one but several (to obtain the mesh boundary fluxes as well as the central average angular fluxes) calculations for each direction, the time required to perform such calculations increases drastically.

In the next section, a study is made of possible methods for reducing the amount of calculational effort required to obtain high order solutions to the transport equation. In addition, several

methods which increase the generality of applications of the discrete ordinates approximation are also investigated. All the methods to be studied are suitable to standard applications of the discrete ordinates approximation as well as to the multiple order quadrature variations presented above [30].

General Quadrature Variations

The calculational effort required to solve higher order approximations to the transport equation using the discrete ordinates method may be prohibitive. In this section some methods which are capable of reducing the number of calculations and, therefore, the machine time, necessary to solve such approximations will be studied.

In a previous section it was shown that invokation of the multigroup formalism yields a system of linear partial differential equations. Due to the nature of these equations, each energy group equation is independent in the sense that it involves only scalar fluxes from the other groups while determining the angular fluxes for that group. According to the iterative process described by equation (25), the major portion of the calculational effort is devoted to successively improved estimates of the scalar fluxes, ϕ_g^{k-1}. While these scalar fluxes depend on the angular flux distribution, equation (22) indicates that a good scalar flux distribution will allow more rapid convergence on the angular fluxes and, thus, on the improved scalar flux, ϕ_g^k, for that group. Since neither angular nor scalar fluxes are known prior to the calculation, it is most common

to use as a first estimate a scalar flux distribution which is constant in the independent variables. This constant value may be zero or may be some value based on the normalization factor to be used. In standard applications of the S_n method, the solution to group g of the multigroup equations

$$|\mathcal{S}_g|\bar{\phi}_g = \bar{S}_g \tag{25}$$

is obtained by using this estimate and iterating on the set of angular flux equations

$$\bar{\Psi} = |\mathcal{A}|\,\bar{\Psi} + \bar{K} \tag{28}$$

for each group until some required degree of convergence is attained. The current scalar fluxes from this calculation are then substituted into equation (25) and the next set of scalar fluxes, for group g+1, determined. The procedure is continued until all group scalar fluxes have been determined. The whole process is then repeated until the multigroup scalar fluxes have themselves converged to the degree required.

In this section, an investigation will be made of alterations to the form of the matrices $|\mathcal{S}|$ and $|\mathcal{A}|$ which will accelerate the convergence process.

Test Configuration

In studying the modifications to be made to the standard discrete ordinates treatment, it is essential that a realistic test configuration

be used. Since comparisons must be made between the various modifications, it is also preferable to use one configuration which may be analyzed by all the variations to be developed.

The configuration chosen is a two space dimension representation of the transverse section of a cylindrical space power reactor shown in figure 13. It is fueled with uranium^{233} nitride and uses lithium^{7} as a coolant. Control is effected by the rotation of two noncentral drums containing boron$_{4}$ carbide and the whole assembly is housed in beryllium oxide which serves as a reflector. It is a typical small reactor with a relatively high median fission energy. The beryllium tends to reduce the energy of the neutrons near the core-reflector interface to allow the much higher low energy boron absorption cross section to be more effective as a control device. The resulting configuration is a severe test of the accuracy of the analysis since it emphasizes both high and low energy fluxes, contains strong absorbers in proximity to thermalizing media and has irregular boundaries.

Eight energy groups, seven fast and one thermal, are used in the analysis. They were obtained by solving the infinite medium transport equation, [31], [32], in the neutron spectrum generated by the appropriate spatial region. The energy range for each group is shown in table 5.

The eigenvalue and flux distribution for this configuration were verified for all the modifications developed. Due to the length of the

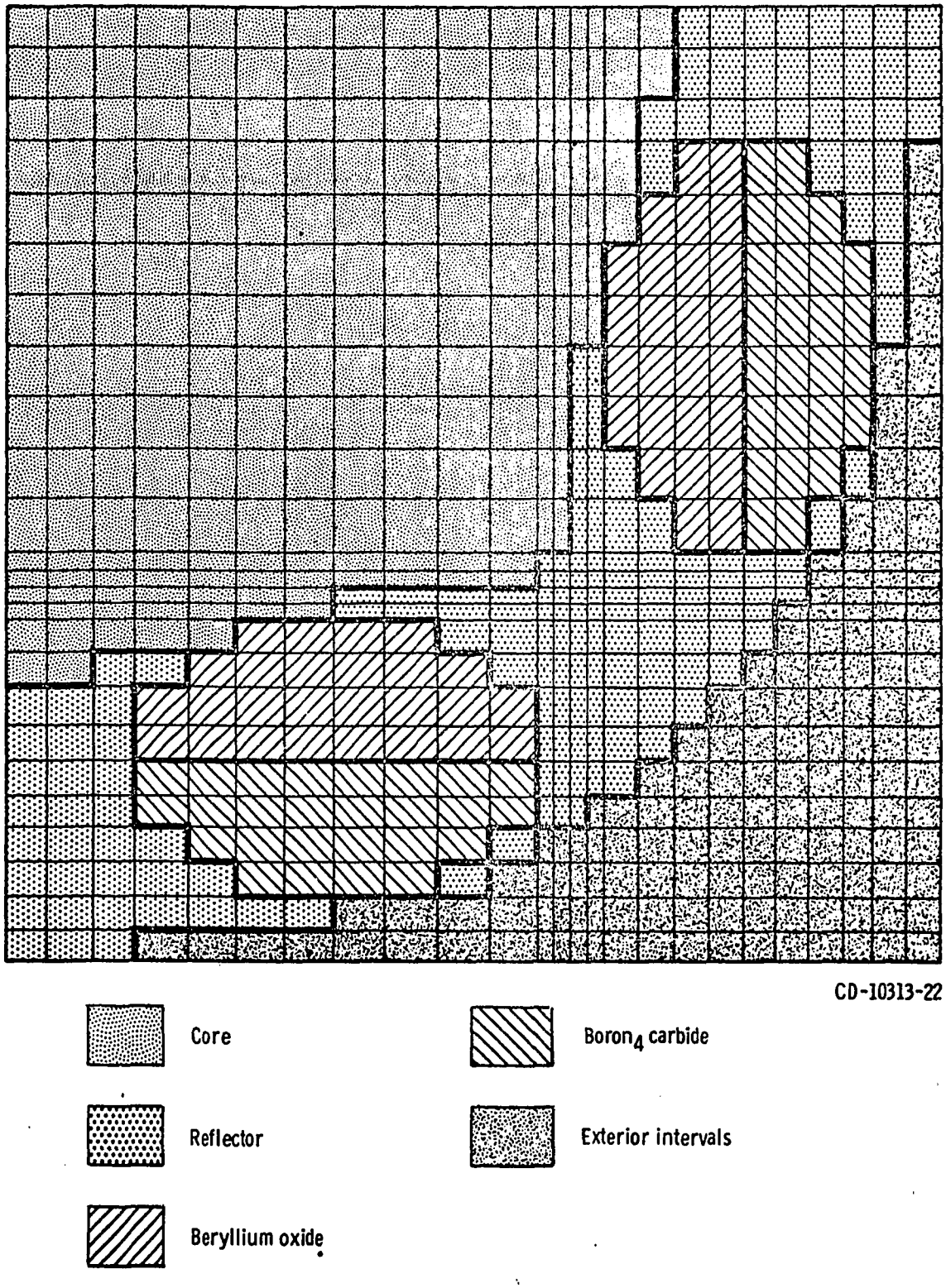

Figure 13. - Spatial and material base case test configuration.

TABLE 5

ENERGY GROUPS AND CROSS-SECTIONS FOR QUADRATURE VARIATION PROBLEMS

Energy Group Boundaries

Energy Group	Upper Bound, eV	Lower Bound, eV
1	14,918, 250.0	820, 850.1
2	820, 850.1	183, 156.4
3	183, 156.4	40, 867.73
4	40, 867.73	15, 034.40
5	15, 034.40	5, 530.846
6	5, 530.846	748.5186
7	748.5186	0.414
8	0.414	0.0253

Material Cross-Sections

σ^a	$\nu\sigma^f$	σ^t	$\sigma_{g,g}$	$\sigma_{g',g}$						
U233 N										
0.0311	0.0736	0.2223	0.1310	0.0000	0.0000	0.0000	0.0000	0.0000	0.0000	0.0000
.0368	.0771	.3067	.2527	.0521	.0000	.0000	.0000	.0000	.0000	.0000
.0452	.0898	.4442	.3912	.0170	.0079	.0000	.0000	.0000	.0000	.0000
.0639	.1251	.5878	.5146	.0073	.0002	.0004	.0000	.0000	.0000	.0000
.0970	.1878	.7133	.6077	.0093	.0004	.0001	.0001	.0000	.0000	.0000
.1527	.2723	1.036	.8816	.0087	.0000	.0001	.0000	.0000	.0000	.0000
.4879	.6119	1.946	1.458	.0017	.0000	.0000	.0000	.0000	.0000	.0000
7.695	16.44	8.037	.3427	.0000	.0000	.0000	.0000	.0000	.0000	.0000
BeO										
0.0030	0.0000	0.2551	0 2024	0.0000	0.0000	0.0000	0.0000	0.0000	0.0000	0.0000
.0000	.0000	.5130	.4471	.0559	.0000	.0000	.0000	.0000	.0000	.0000
.0000	.0000	.5772	.5065	.0659	.0002	.0000	.0000	.0000	.0000	.0000
.0000	.0000	.6070	.4944	.0707	.0000	.0000	.0000	.0000	.0000	.0000
.0000	.0000	.6088	.4559	.1126	.0000	.0000	.0000	.0000	.0000	.0000
.0000	.0000	.6184	.5615	.1128	.0000	.0000	.0000	.0000	.0000	.0000
.0001	.0000	.6170	.6047	.0569	.0000	.0000	.0000	.0000	.0000	.0000
.0007	.0000	.6451	.6443	.0150	.0000	.0000	.0000	.0000	.0000	.0000
B_4C										
0.0253	0.0000	0.2402	0.1743	0.0000	0.0000	0.0000	0.0000	0.0000	0.0000	0.0000
.0759	.0000	.4929	.3539	.0407	.0000	.0000	.0000	.0000	.0000	.0000
.2330	.0000	.6042	.3328	.0631	.0001	.0000	.0000	.0000	.0000	.0000
.4339	.0000	.7302	.2385	.0385	.0000	.0000	.0000	.0000	.0000	.0000
.7106	.0000	1.167	.3570	.0579	.0000	.0000	.0000	.0000	.0000	.0000
1.485	.0000	2.007	.4710	.0990	.0000	.0000	.0000	.0000	.0000	.0000
25.73	.0000	26.25	.5064	.0503	.0000	.0000	.0000	.0000	.0000	.0000
355.7	.0000	364.9	9.243	.0132	.0000	.0000	.0000	.0000	.0000	.0000

1. In the scattering matrix, g' runs g, g-1, g-2, . . ., g-7.

2. Fission fractions (χ_g) are 0.7491, 0.2176, 0.0303, 0.003, 0.0, 0.0, 0.0, and 0.0.

high order (S_8 and S_{16}) calculations in some of the optimization studies, a one dimensional representation of the reactor was used.

Angular Quadrature Variations

In this section only techniques which alter the form of the multigroup matrix $|\mathcal{A}|$ will be considered. In the procedure outlined in the introduction the matrix equations for the angular fluxes

$$\overline{\Psi} = |a|\ \overline{\Psi} + K \tag{28}$$

in each group are solved completely for each direction in a high order quadrature before the next iteration on the scalar flux matrix, $|\mathcal{A}'|$ in accordance with equation (34)

$$\overline{\phi} = |\mathcal{A}'|\ \overline{\phi} + \overline{S}' \tag{31}$$

is performed. In this process, a large number of unnecessary calculations are performed since, particularly in the early outer iterations, the scalar fluxes vary rapidly. The variation is due to the initial poor estimate of the scalar flux distribution used for the source, SV, terms in equation (22). These rough scalar fluxes control the angular flux calculation and, therefor, the next iterative value for the scalar fluxes. The whole iterative process would be accelerated if a procedure for obtaining more rapid early estimates were developed.

One method for such an accelerative procedure may be derived using one of the results of Cesari's algorithm presented in the Introduction in this chapter. In the three term representation of the series solution

$$\overline{\phi} = \overline{\phi}_1 + \overline{m}_1 + \overline{\phi}_2 \tag{32g}$$

to the problem stated by equation (32a), where $|m|$ represents the high order quadrature matrix desired for the final solution, it was shown that the residue term is small if the approximate matrix, $|\eta|$, used in finding

$$\bar{m}_2 = \left(|m| - |\eta|\right)\left(\bar{\phi}_1 + \bar{m}_1\right) \tag{32f}$$

is close to $|m|$. Rather than use the series solution for $\bar{\phi}$, which is limited in application for the reasons given previously, use will be made of the fact that succeeding discrete ordinates angular quadratures are relatively close in form. That is, an S_{n+2} quadrature contains few additional characteristic directions and, in general, yields a flux distribution similar to that of an S_n quadrature. Then, for the S_{n+2} and S_n matrices

$$\bar{m}_2 = \left(|\eta_{S_{n+2}}| - |\eta_{S_n}|\right)\left(\bar{\phi}_1 + \bar{m}_1\right) \tag{39}$$

The residue term will then be small if

$$|\eta_{S_{n+2}}| \rightarrow |\eta_{S_n}|$$

and, therefore, the differential scalar flux, $\bar{\phi}_2$, of equation (32g) should be small. The scalar flux obtained by solving

$$\bar{\phi}_n = |\delta_n|\,\bar{\phi}_n + \bar{S}_n$$

will then constitute an accurate estimate for the matrix problem

$$\bar{\phi}_{n+2} = |\delta_{n+2}|\,\bar{\phi}_{n+2} + \bar{S}_{n+2}$$

so that the solution, $\bar{\phi}_{n+2}$, may be much more rapidly obtained. In

accord with equation (39), only quadrature orders which are relatively close in form may be used. The final solution, therefore, must be approached by the application of successively ascending quadrature matrices to $|\mathcal{A}'|$ in equation (31). That is, rather than approximating the solution to the angular quadrature order $\dot{N}$ problem

$$\overline{\phi} = |\mathcal{A}_N|\ \overline{\phi} + \overline{S} \tag{31}$$

by the series

$$\overline{\phi}_N = \sum_{n=1}^{N-1} \left(\overline{\phi}_n + \overline{m}_n\right) + \overline{\phi}_N \tag{32m}$$

The true solution to that problem will be found by the successive application of progressively higher order angular quadratures.

In the implementation of this method, several considerations are of importance. Since the accuracy of each succeeding approximation to the final order quadrature is not known in advance, provision must be made for allowing any progression of quadratures to be used. To avoid unnecessary calculations, several arbitrary termination criteria for each quadrature step should also be incorporated. Such provisions will not only allow studies to be made of the optimum manner in which to approach convergence on the final quadrature but will also reduce or eliminate the application of angular quadratures where each step in the progression $n \rightarrow n+2$ is not required due to similarity of the solutions in the lower order sets. As the multigroup equations directly use only the scalar fluxes, it is also possible to use $|\alpha|$ matrices corresponding to different order final quadratures in various energy groups. Since

most configurations involve energy dependent cross sections in which the optimum quadrature would not be the same for all groups, an option for permitting the quadrature order to be a function of energy is included.

Since the lower order quadratures cannot be expected to yield scalar flux distributions with an accuracy equivalent to that of higher order quadratures, there is little point in solving the lower order calculation to the same degree of convergence required for the final calculation. The major benefit in the final calculation should be derived from the use of intermediate scalar flux estimates which minimize the number of inner iterations required for convergence on the final quadrature and not from fully converged low order scalar fluxes. An important question in this regard is that of determining the optimum point at which to effect the quadrature variations. In order to investigate the effect on solution time of the variations discussed, the discrete ordinates approximation has been programmed to permit the following sequences of operation:

(1) The use of any number of preliminary lower order angular quadrature sets. The progression may involve each succeedingly higher order set or allow the omission of specified orders in the progression.

(2) The termination of the calculation on a given quadrature set either by completion of a number of outer iterations or by attainment of some specified intermediate degree of convergence.

(3) The execution of a number of outer iterations on a given quadrature set terminated by prior intermediate convergence on that set.

(4) The final angular quadrature order to be made a function of the energy group in the problem. This feature may be applied in conjunction with the preliminary lower order quadrature sets.

Sequences (2) and (3) imply that more than one degree of convergence may be used on the same quadrature set. In effect, this serves to limit the number of inner iterations on the angular flux matrix (28) in the early phases of the calculation. In addition, all options normally used in S_n applications, including additional convergence tests and acceleration procedures, are retained. None of the modifications made which involve varying the angular quadrature order during the course of the calculation should affect the accuracy of the final results. Convergence on the final values of the angular fluxes, eigenvalues, and other quantities must not depend on the manner in which the calculation is begun. This is also true, within the framework of the quadrature orders used, for the modification in which the quadrature is made a function of the energy.

In order to study the effect of the various permutations of options (1) through (4), a one dimensional representation of the test configuration previously described was used. Since the primary consideration, in addition to verifying the accuracy of the solution, is to develop a procedure for approaching final convergence, two test cases have been used. They differ only in the order of the final angular quadrature. The first uses an S_8 final approximation and the second an S_{16} final set. The purpose is to observe the optimum manner in which to approach final convergence in intermediate order (S_8) and higher order (S_{16}) calculations. The results are presented in tables 6 and 7. The headings in these tables are self-explanatory. In case (f) of table 6, for example, two preliminary quadratures, S_2 and S_8, were used although the latter (S_8) is identical to the final. The 2ϕ

TABLE 6

ANGULAR QUADRATURE VARIATIONS

Test[1] Case	Preliminary Angular Quadratures	Quadrature[2] Variation Criterion	Solution[3] Time	Eigenvalue[4]
a.	S_2	2φ	0.751	1.6051
b.	S_2	3φ	.727	1.6051
c.	S_2	10^{-2}	.644	1.6051
d.	S_2	10^{-3}	.700	1.6051
e.	S_2	10^{-4}	>1.000	------
f.	S_2, S_8	2φ, 10^{-2}	.601	1.6051
g.	S_2, S_8	2φ, 10^{-3}	.478	1.6051
h.	S_2, S_4	2φ, 10^{-3}	.672	1.6051

[1]Base test case is standard S_8 angular quadrature requiring 2.53 minutes for final solution.

[2]$n\varphi$ is the number of outers run on the indicated quadrature set. Other criteria refer to maximum allowable change of self-scattering term in sequential iterations.

[3]Solution time is given in fractions of base case solution time.

[4]The commonly used term "Eigenvalue" is actually the reciprocal of the eigenvalue ($1/\lambda$).

TABLE 7

ANGULAR QUADRATURE VARIATIONS

Test[1] Case	Preliminary Angular Quadratures	Quadrature[2] Variation Criterion	Solution[3] Time	Eigenvalue[4]
a.	S_2, S_4, S_8	2φ, 4φ, 10^{-3}	0.427	1.6052
b.	S_2, S_{16}	4φ, 10^{-3}	.514	1.6052
c.	S_2, S_4, S_8	10^{-4}, 10^{-4}, 10^{-4}	.590	1.6052

[1]Base test case is standard S_{16} angular quadrature requiring 9.33 minutes for final solution.

[2]As in Table 6. Where multiple preliminary quadratures are used, the Quadrature Variation Criteria are applied in the order listed.

[3]As in Table 6.

[4]As in Table 6.

indicates that two outer iterations were first performed using an S_2 quadrature. The first S_8 calculation, as indicated in the Quadrature Variation column, is converged to a lesser degree than the final calculation to limit the number of inner iterations. The Solution Time is the time required to attain final convergence. As may be seen, all the modifications return the same eigenvalue in the final calculation.

For the test case used, with final quadratures of S_8 or lower order, the maximum time reduction is obtained when only a single preliminary S_2 calculation is performed. For problems involving quadratures of higher order than S_8, the optimum approach is to use more than one preliminary quadrature. This is best illustrated, for the S_8 or lower quadratures, by case 1h which uses both an S_2 and S_4 preliminary calculation and whose running time to final convergence exceeded that of case 1g which had only an S_2 start. For an S_{16} final quadrature, however, case 2b, which used only an S_2 preliminary calculation, required considerably longer to converge than case 2a, which used successively higher quadratures to approach final convergence.

For those problems in which the use of only a single preliminary quadrature is most efficient, a number of trial cases (1a to 1g) were run in order to determine when to shift from the preliminary to the final quadrature. As discussed previously, full convergence on the preliminary quadrature is probably not desirable. This is borne out by case 1e of table 6 which converged the S_2 start to the final (10^{-4}) criterion and required more running time than any of the other methods applied. These cases also indicate that final convergence is best approached by first performing several outer iterations and then

converging to some intermediate criterion on the final quadrature. The use of this intermediate criterion essentially acts to limit the number of inner iterations per outer iteration during that portion of the calculation when the flux distribution is changing rapidly. The same effect could be achieved by directly controlling the number of inner iterations per outer iteration but this procedure affords no way of insuring that the flux in each energy group is equally well converged. Case 1g, which used this approach, yielded the shortest running time for the problem.

For those problems in which multiple quadratures are used to approach final convergence, it is more difficult to specify an optimum approach. The calculation of all of the large number of permutations afforded by allowing both a given number of outer iterations and an intermediate convergence for each quadrature criterion would require an inordinate amount of effort. Again, however, case 2c of table 7 demonstrates that running to full convergence on each preliminary quadrature is less efficient than use of other available options. Consideration of the results of the cases run shows that the shortest running time for the S_{16} solution was achieved by performing a limited number of outer iterations on both an S_2 and an S_4 preliminary calculation followed by intermediate convergence on an S_8 quadrature and, finally, by final convergence on the S_{16} solution. Case 2a, which followed this pattern, reduced the time required to obtain an S_{16} result by more than fifty percent.

The program modification which allows the quadrature order to be specified by energy group was also tested on the same base case but with

the quadrature sets for the eight energy groups arbitrarily chosen as $2S_8$, $4S_4$, and $2S_2$ starting with the highest energy group. For this test case the running time was reduced by about sixty percent. The low order quadrature start may also be used in conjunction with this modification to further reduce the running time. The value of this modification is limited due to the difficulty involved in specifying appropriate quadrature orders.

Spatial Quadrature Variations

Present applications of the discrete ordinates method require that a uniform spatial mesh be employed. This means that the interval spacing used in one direction must be retained over the whole configuration. For example, the use of rectangular coordinates to represent the cylindrical boundary shown in figure 13 requires the retention of extraneous intervals lying outside the actual configuration. The typical reactor problem also contains larger homogeneous regions which should not require the same detailed spatial treatment as is necessary near material interfaces or boundaries. Since the angular flux matrix, $|a|$, must be repetitively computed for each mesh iteration, reduction or elimination of unnecessary intervals would improve the efficiency of the calculation. Another desirable option would be to obtain an initial improved flux estimate by first solving a less detailed problem.

Although the work performed in this section involves the angular flux equations,

$$\overline{\psi} = |a| \, \overline{\psi} + \overline{K} \tag{28}$$

the form of the equations is unchanged. The alterations involved are

essentially calculational in nature and involve the process in which the equations are applied to the spatial mesh. That is, terms a_{ij} of the matrix $|a|$ and the vector $\overline{K}$ are made a function of the spatial mesh interval. The arguments given above indicate that there are three major variations to the standard application of the discrete ordinates approximation which would reduce the required number of calculations.

(1) An option for specifying the number of intervals in each row and column of the spatial mesh matrix should be added. This option retains the standard mesh spacing but permits the rows and columns to be truncated. This provision should also allow the use of any of the standard boundary conditions on any surface of the configuration, whether truncated or not. The particle leakage given by integrating the angular fluxes over the truncated surfaces must also be correctly calculated.

(2) An option for varying the mesh interval spacing, in any direction, of interior regions of the configuration is required. In effect, this allows several intervals, in regions where little variation in the angular flux is anticipated, to be combined. The angular flux matrix must then be solved only once rather than for each original interval. One problem connected with this option is the specification of the angular flux values at interfaces between the normal and reduced spatial meshes. Since this option is intended for use only in regions where the flux variation is not severe, the assumption is made that the angular flux on the reduced boundary is the average of the angular fluxes entering through the interface. For example, if there are K intervals bordering one reduced interval, the angular flux at the boundary is

$$\psi_m = \sum_{k=1}^{K} \psi_{m,k}/K$$

When crossing the interface in the opposite direction, the angular flux in each normal interval is taken to be equal to that at the reduced boundary

$$\psi_{m,k} = \psi_m \qquad (k=1,2,\ldots K)$$

(3) Since one criterion for all the variations under consideration is that they be capable of returning solutions identical to that of the standard method, a provision for expanding the scalar flux vectors obtained in (1) and (2) to match the original spatial configuration is included. This permits further convergence to the standard solution for the original mesh and also allows accurate comparison of solution times.

The first modification tested was that in which the number of intervals in each row and column is allowed to vary. This option is primarily useful where it is necessary to use rectangular coordinates to analyze a cylindrical core such as shown in figure 14. Any combination of the normal boundary conditions is permitted so that the quarter, half, or full configuration may be run. In the standard S_n treatment, it is necessary to run the complete rectangular mesh with some artificial material in the extraneous intervals. It is possible to compare the accuracy of this modification with that of the standard treatment by inserting a "perfect absorber" into these intervals. Comparison of the eigenvalues from such calculations shows agreement, at the end of each outer iteration, to better than the accuracy required by the convergence

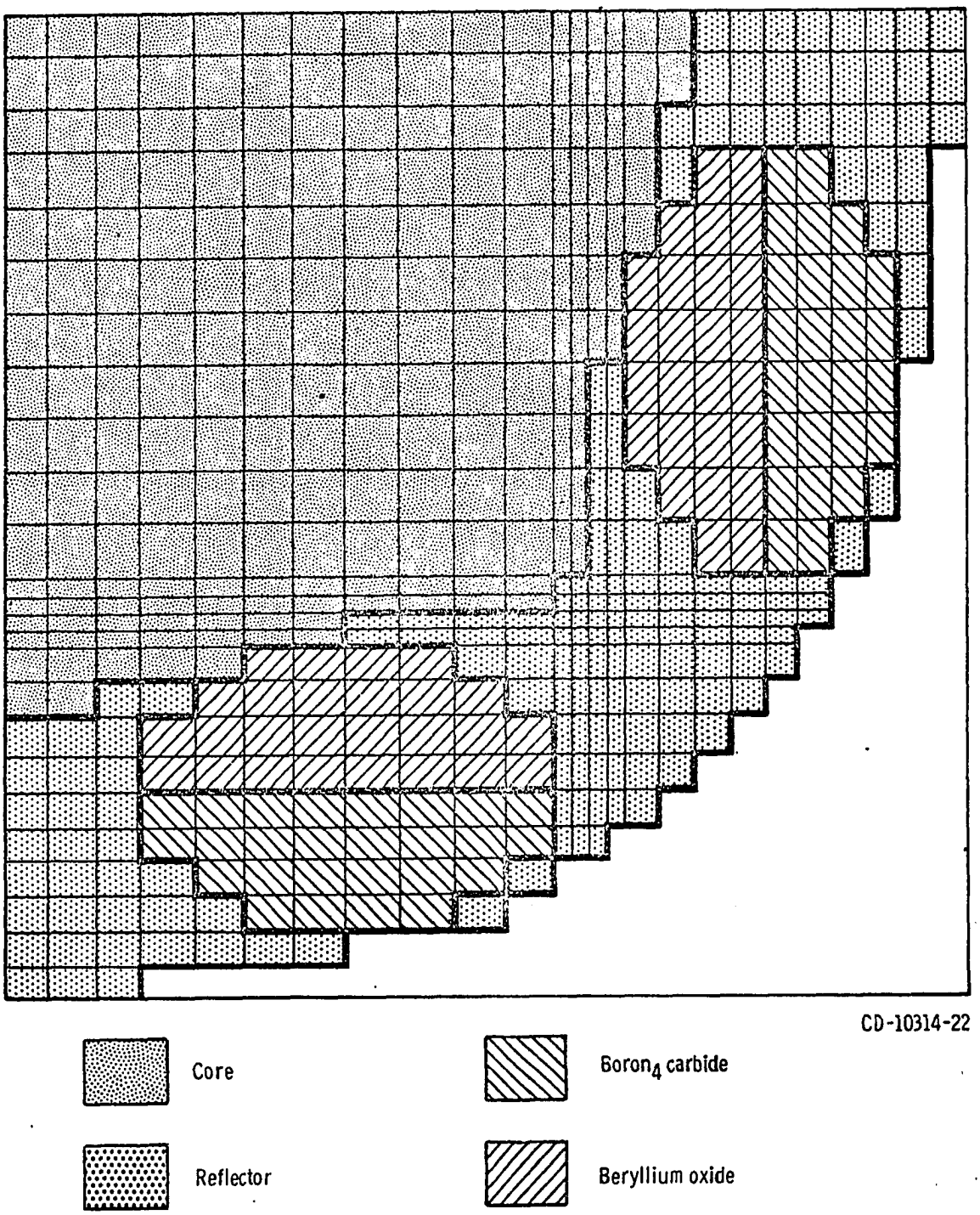

Figure 14. - Spatial mesh (interval truncation) variation.

criterion used. The time reduction depends, of course, on the complexity of the original case and on the number of intervals deleted. For the configuration of figure 14, with the exterior intervals removed from the computation, the time reduction is approximately 25 percent.

As a test of the leakage calculation, a simple case was run using cylindrical coordinates in a standard S_n code to obtain the eigenvalue and leakage for a 10 centimeter radius cylinder with no internal details. This run was then compared with the interval deletion modification results using a ten interval approximation of the cylindrical boundary. The comparison yields

	Eigenvalue $(1/\lambda)$	(Leakage)/(Source Neutron)
Original TDSN	0.9623	0.0377
Interval deletion	.9617	.0383

which is quite accurate since only ten steps were used to approximate the boundary.

The second modification, in which interior mesh intervals within homogeneous regions of the core are combined, is the most complex in terms of alternations made to the standard flow. Since the method of implementing any such scheme is quite arbitrary, a brief description of the procedure followed will be given.

The normal spatial mesh is first defined. Two interior coordinate boundaries are then specified. Within these boundaries, the interval reduction, or combination, may be applied. Each original region is comprised of a given number of intervals, bounded by mesh lines. The interval reduction is accomplished by choosing the number of mesh lines,

in each direction, to be eliminated. Thus, sets of from one to the total number of interval lines may be removed. As an example, if sets of two are removed, two interval boundaries are deleted, the next is retained, the next two removed and the process continued until the outer region boundary is reached. This process is illustrated in figure 15. The elimination is performed independently in each coordinate direction with the only restriction being that the last remaining interval boundaries must coincide with the original region boundaries. Figure 16 indicates the results of applying this process to the test case. Since the process results in dissimilarly sized adjacent intervals, the assumption made concerning the behavior of the angular fluxes across such boundaries is applied.

As an example of the use of this modification, the configuration shown in figure 16 was run with the intervals combined as indicated. This problem should represent an extreme test of the modification since some intervals have been combined in regions, such as near the control drums and material interfaces, where the angular fluxes are expected to vary rapidly. Two test cases were run and compared with the results of the original version of the program in order to compare both eigenvalues and reactivities. The second case is also as in figure 3 but with the control drums rotated 90° clockwise. Results for the first case are

Method	Time (min)	Eigenvalue ($1/\lambda$)
Standard S_n Code	17.22	1.285
Interval reduction	11.96	1.280

1. In R_1, one set of 2 interior boundaries is removed.
2. In R_2, three sets of 1 interior boundary are removed.
3. The resulting mesh retains only the boundaries x_0, x_3, x_5, x_7, and x_9 within the horizontal limits specified.

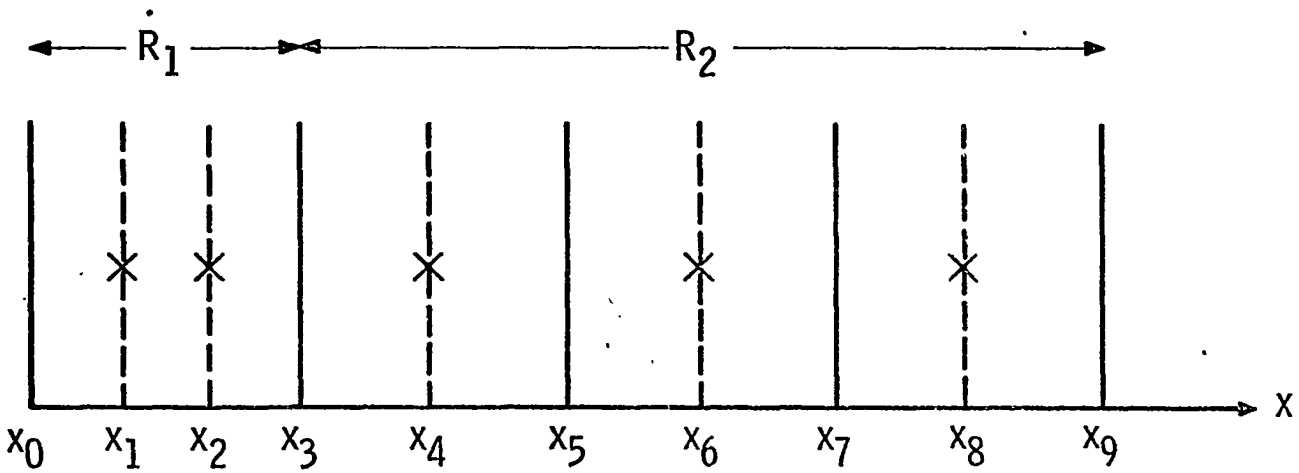

Figure 15. - Spatial mesh (interval combination) example.

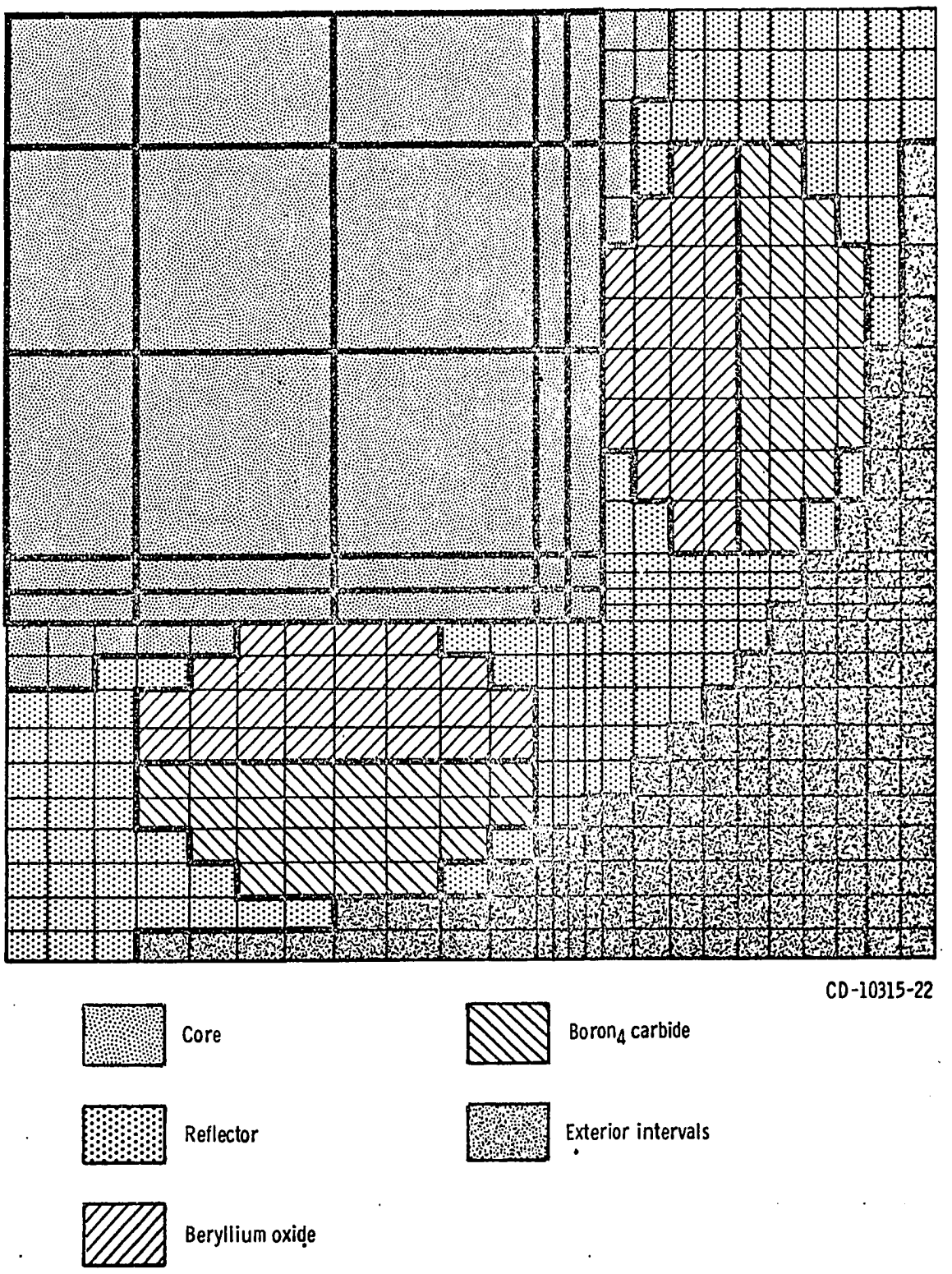

Figure 16. - Spatial mesh (interval combination) variation.

and the eigenvalues differ by 0.39 percent. The running time is reduced by about 35 percent.

For the 90° control drum rotation, the results are

Method	Time (min)	Eigenvalue ($1/\lambda$)
Standard S_n Code	22.88	1.256
Interval reduction	15.44	1.252

and the eigenvalues differ by 0.32 percent with a time reduction of about 33 percent. A comparison of the control reactivities shows that the original version yields 2.28 percent $\delta k/\bar{k}$ and the interval reduction scheme 2.21 percent $\delta k/\bar{k}$. This is good agreement in view of the fact that intervals have been deleted in regions where the flux does not conform to the assumption of relative constancy.

The most general application of this variation is to generate a preliminary scalar flux guess for use in a final calculation over the original spatial mesh. To demonstrate this, a configuration similar to that shown in figure 16 was run, using a coarse spatial mesh with less detail in the control drum region, for three outer iterations of the reduced mesh. The scalar fluxes resulting from this calculation were then expanded to fit the original mesh, and the final iterations converged on this mesh. A comparison of the times involved yields

Method		Time (min)	Eigenvalue ($1/\lambda$)
Original S_n Code		13.32	1.145
Interval Reduction	Coarse mesh	4.192	1.135
	Original mesh	+3.830	1.145
		=8.022	

for a time reduction of approximately 40 percent.

The variations described above, which affect the application of the angular flux equations to the spatial mesh, are seen to be capable of significantly reducing the calculational effort required in applications of the discrete ordinates approximation. While the variations which allow deletion and combination of spatial mesh intervals are applicable only to configurations satisfying certain conditions, such cases are fairly typical in both reactor and shield design. The test case used is an example of a problem which is most suited for analysis in Cartesian coordinates and profits from the elimination of extraneous intervals. In addition, all variations yield scalar flux estimates which are rapidly obtained and accelerate convergence of the original problem.

CHAPTER V

VERIFICATION OF NUMERICAL METHODS

In this chapter, the validity of the numerical methods developed in the preceding sections will be verified. While the techniques developed in this paper will be employed to accelerate convergence of the problems considered, the primary purpose is to insure that the inclusion of these techniques has not disturbed the convergence properties of the discrete ordinates approximation and that the accuracy of the numerical methods is acceptable.

The choice of problems to be used in accomplishing these ends is of considerable importance. While the analysis of experimental data constitutes one class of problem which may be compared to the numerical solution, the lack of accurate experimental cross-section data and the necessity for approximating experimental geometries with orthogonal coordinate meshes make exact comparisons impossible. As discussed in Chapter II, however, it is possible to obtain exceedingly accurate analytic solutions to certain simple classes of problem. One of the quantities which may be most accurately determined in such problems is the critical radius of homogeneous configurations. A considerable amount of effort has been expended by Carlson and Bell [33] in determining exact critical radii for slabs, spheres, and cylinders. The results obtained incorporated data taken from Case, de Hoffmann,

and Placzek [34] and used a variety of methods to insure accuracy to four decimal places.

One of the major drawbacks in using the results of such problems to verify the numerical methods developed is that, due to analytic restrictions and the calculational effort involved, solutions to such problems are based on one-group theory. Some essential features of the numerical methods, such as the treatment of the source terms (the full inter-group scattering matrix and the allocation of fission neutrons) in equations (24d) and, subsequently, (25), are then, not tested. However, in the following section, a procedure for eliminating this defect is given and some multigroup, rigorously soluble, test problems developed.

Multigroup Test Problems

Of the range of problems for which rigorous monoenergetic critical radii are available, both the infinite slab and the sphere represent one dimensional calculations. Since one purpose of the test case is to verify the multidimensional calculation, the right circular cylinder will be used as a test configuration. While the exact solutions referenced are for infinite cylinders, there are several ways in which the results may be extended to two spatial dimensions. For the test problems below, an r-θ geometry will be used. This configuration is as shown in the sketch on the next page and provides a severe test of the ability of the approximation to calculate particle flux redistribution across the faces of the mesh intervals. Rather

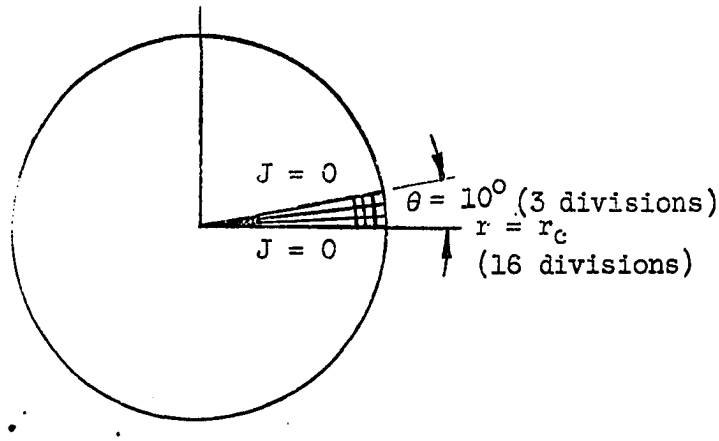

than calculate the complete 360 degree mesh, the numerical perfect reflection boundary condition (in which the net current is zero) will be applied to the vertical boundaries as also shown above. The standard geometry will then be defined as having 16 intervals in the r direction and 3 intervals in the θ direction, subtending a 10 degree arc.

In order to extend the monoenergetic results to multigroup problems, a device developed by this author [35] will be introduced. This procedure involves the definition of c, the number of particles released per collision by the target medium. For a fissionable material

$$c = \frac{\nu\sigma^f + \sigma^s}{\sigma^t} \tag{40}$$

This definition will be extended by redefining the number of particles per collision for a multigroup problem as

$$c = \frac{\nu_g \sigma^f_g + \sum_{g'}^{G} \sigma^s_{gg'}}{\sigma^t_g} \tag{41}$$

where, again, g is the group index and G the total number of groups. As an example, for a value of c equal to 1.2, the one group cross-sections would be

$$c = \frac{0.2 + 1.0}{1.0} = 1.2$$

Use of equation (41), however, allows formation of the following scattering matrix

THREE GROUP CROSS-SECTIONS

c = 1.20							
σ^a	$\nu\sigma^t$	σ^t	$\sigma_{g+2,g}$	$\sigma_{g+1,g}$	$\sigma_{g,g}$	$\sigma_{g-1,g}$	$\sigma_{g-2,g}$
0.0	0.2	1.0	0.3333	0.3333	0.3333	0.0000	0.0000
0.0	0.2	1.0	0.0000	0.3333	0.3333	0.3333	0.0000
0.0	0.2	1.0	0.0000	0.0000	0.3333	0.3333	0.3333

for a three energy group expansion. It should be noted that this set of cross-sections, which will be used in the test problems, rigorously tests the fission production and energy exchange between groups. Since the scattering matrix creates a perfect balance between energy groups, it is only necessary to alter the value of $\nu_g \sigma^f_g$ to obtain the desired value of c.

The value of c determines not only the critical radius but also the character of the problem. That is, as the c value is increased (corresponding to a more enriched reactor), the critical dimensions of the system are reduced. For small c (or large radius), the problem closely corresponds to a diffusion problem. For larger c (and small radius), the boundary effects exert more influence and higher order transport approximations may be required. In order to test the ability of the numerical procedure at both ends of this range, the test problems include the smallest and largest values of c for which an exact solution is available. Since primary interest is in eigenvalue problems, the c value is required to be larger than one. Three test cases are calculated: the first has $c = 1.02$ and a critical radius of 9.0433 centimeters, the second has $c = 1.2$ with a 2.2884 centimeter radius, and for the last $c = 2.0$ and the radius is 0.6673 centimeters.

Test Problem Convergence

Prior to correlating analytical and numerical results, it is necessary to specify the degree of accuracy to be required on the numerical solutions. The general question of the existence and uniqueness of such solutions has been well investigated [36][37]. A more recent paper [38], containing a bibliography, discusses the subject with respect to the generalized transport equation under certain finite difference approximations. Since the subject is lengthy and difficult to treat in a limited space, the following discussion is predicated on the existence of such solutions.

Given an appropriate solution, the fundamental problem in any iterative procedure is specifying the accuracy to which the solution is to be found. In particular, this requires the application of some convergence criteria to one of the computed quantities. Since the difference equations formulated are used to determine the flux distributions, it is most convenient to apply criteria to these eigenvectors. In most practical applications, it is the scalar fluxes which are of greatest interest so that, in the work performed, all convergence tests will apply to quantities directly associated with these fluxes.

There are many variations of convergence tests, using these scalar fluxes, which may be applied. For example, the scalar flux, ϕ^k, in the k^{th} iteration may be compared with that, ϕ^{k-1}, of the previous iteration and the difference required not to exceed some given limit. If this criterion is applied to each spatial mesh interval, the test is generally too restrictive since there are usually some space points which converge slowly but are relatively unimportant insofar as the overall calculation is concerned. On the other hand, integral tests (i.e., comparing the flux integrals in each group) may not be sufficiently accurate. The convergence tests used in this work are all based on the use of one criterion, ε. In order to insure that both the inner and outer iterations are converged several tests are applied. These represent a combination of both point and integral (summation) quantities in successive iterations. Using the notation previously developed, the following quantities are tested. The individual factors in the formulas represent values in each mesh interval

and the spatial subscripts are dropped to simplify the notation. For inner iterations:

1. The ratio of the largest in-group scattering (by spatial interval) to the integrated group flux (for the whole configuration)

$$\frac{\left|\sigma^{s}_{g\to g}\left(\phi^{k}_{g} - \phi^{k-1}_{g}\right)V\right|}{\sum_{i,j,k} \phi^{k}_{g} V}$$

2. The ratio of the integrated change in in-group scattering to the integrated group flux

$$\frac{\sum_{i,j,k} \left|\sigma^{s}_{g\to g}\left(\phi^{k}_{g} - \phi^{k-1}_{g}\right)V\right|}{\sum_{i,j,k} \phi^{k}_{g} V}$$

3. The ratio of the integrated change in the group removal to the integrated group flux

$$\frac{\sum_{i,j,k} \left(\sigma^{t} - \sigma^{s}_{g\to g}\right)\left(\phi^{k} - \phi^{k-1}\right)V}{\sum_{i,j,k} \phi^{k} V_{tot}}$$

Each of these quantities must satisfy the convergence criterion in each energy group.

For the outer iterations:

1. The ratio of the change in the total integrated scattering

loss to the total integrated flux

$$\frac{\sum_{g}\sum_{i,j,k}\left(\sigma_{g}^{s}\phi^{k-1}V\right)}{\sum_{g}\sum_{i,j,k}\left(\sigma_{g}^{s}\phi^{k}V\right)}$$

2. If up-scattering is present (as in the test problems) the ratio of the change in the total integrated up-scattering to the total integrated flux

$$\frac{\sum_{g}\sum_{i,j,k}\sigma^{up}\left|\phi^{k}-\phi^{k-1}\right|V}{\sum_{g}\sum_{i,j,k}\phi^{k}V}$$

3. The effective multiplication factor, k_{eff}, in three successive outer iterations (to prevent fortuitous convergence) is compared

$$\left|k_{eff}^{k}-k_{eff}^{k-1}\right| \quad \text{and} \quad \left|k_{eff}^{k+1}-k_{eff}^{k}\right|$$

Each of these quantities must satisfy the convergence criterion in each outer iteration (over all energy groups).

These convergence tests are applied in the test problems developed above. In general, all these problems were solved using a convergence criterion, ε, of 0.0001. Based on previous experience, it is anticipated that the results obtained (the effective multiplication factors) will be accurate to at least three decimal places. Since the exact multiplication factor is unity, the solutions should be comparable to tenths of a percent.

Numerical Methods Comparison

Since the exact critical radius is known, the procedure used in these cases will be to determine the eigenvalue (and effective multiplication factor, k_{eff}) for the given cross-section set in ascending quadrature orders. The general criterion on the numerical solutions will be an error of about one-tenth of a percent in the multiplication factor. This procedure also allows some insight into the quadrature order required to obtain the specified criterion.

The results obtained from the various calculations are collected in table 8. As may be seen, it is possible to approach the exact result in all cases by refining the angular quadrature mesh. It should be noted that, as anticipated, relatively higher order quadratures are required in the cases where transport effects assume more importance. This is illustrated in figure 17 where the approach to convergence of the most difficult transport problem ($c = 2.0$) has been plotted as a function of ascending angular quadrature order. While the discrete representation of the remaining variables precludes calculation of the exact result, it is seen that the higher quadrature orders (S_8 through S_{12}) represent a slowly convergent process toward this result. This graph also indicates the necessity for using higher order angular quadratures than are normally employed in such calculations.

The accuracy of the results obtained in these cases demonstrate the validity of the discrete ordinates approximation and of the coding developed to implement it. The quadrature detail required also emphasizes the importance of the quadrature variations developed in the preceding chapters.

TABLE 8

[1]CALCULATION OF EXACT CRITICAL RADII

Case Number	Quadrature Order	c Value	Critical Radius	k_{eff}
1	S_2	1.02	9.0433	1.012090
2	S_4	1.02	9.0433	1.001075
3	S_2	1.20	2.2884	0.999407
4	S_4	1.20	2.2884	1.011786
5	S_6	1.20	2.2884	1.006326
6	S_8	1.20	2.2884	1.001433
7	S_2	2.00	0.6673	0.948277
8	S_4	2.00	0.6673	1.006967
9	S_6	2.00	0.6673	1.008812
10	S_8	2.00	0.6673	1.006309
11	S_{10}	2.00	0.6673	1.003868
12	S_{12}	2.00	0.6673	1.002586

[1]For the exact critical radius given, the eigenvalue should be identically 1.0.

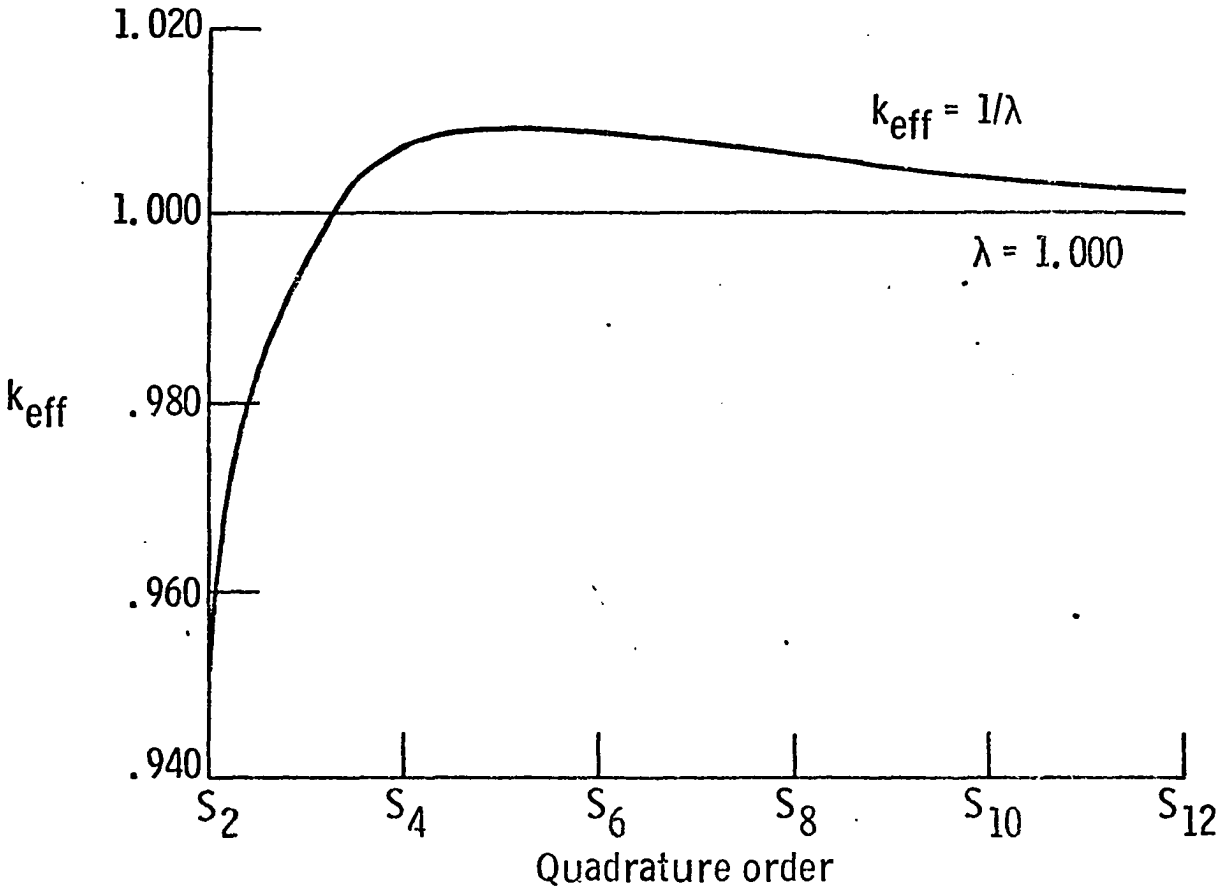

Figure 17. - Approach to exact eigenvalue through ascending quadrature orders.

CHAPTER VI

DISCUSSION OF RESULTS AND CONCLUSIONS

Discrete Ordinates Codes

The Boltzmann transport equation, in a form suitable for describing the behaviour of non-mutually interacting particles in a medium having specified nuclear properties, may be applied to a wide variety of problems. Among these are radiative transfer in stellar atmospheres, neutron flux distributions in critical assemblies, and photon transport in shielding materials. Representative problems in these fields are normally complex and solutions require the use of numerical methods in conjunction with digital computer machinery. The most successful numerical method yet developed for such problems is the discrete ordinates approximation to the transport equation.

The widespread application of S_n techniques is apparent in the number of machine codes currently in use. The design of newer machine programs typically extends the range of possible discrete ordinates solutions. Thus, recent codes are spatially multidimensional [16], solve the time dependent transport equation [39], permit various auxilliary calculations [40] (i.e., critical radius or concentration searches), and treat anisotropic scattering [41] and [42].

The present generation of computer machinery is capable of processing almost arbitrarily large problems. One of the inherent

restrictions of the S_n method is the need for detailed energy, space, and angular quadratures to insure adequate accuracy in the solutions. The most serious problem associated with the application of computers to these detailed problems is the inordinately large amount of machine time required to converge the iterative process. It is not unusual for the typical multidimensional representation of a reactor design to require several hours to converge. Discovery of the fact that lower order angular quadratures may not yield precise results will also tend to increase the size of the average problem. Such calculations rapidly become prohibitive in terms of machine utilization and cost.

Reduction of Solution Time

This study has been made to investigate various means for reducing the calculational effort required to obtain solutions for the discrete ordinates approximation to the transport equation. Some of the methods developed may also be used to extend the range of application of S_n techniques in certain classes of problems. The methods developed rely on the general principle of permitting variations in the angular and spatial quadratures to be made during the course of the iterative procedure. In addition, the methods are general in the sense that they are directly applicable to all coordinate systems and may be used in conjunction with any numerical techniques for solving the discrete ordinates approximation.

Machine Configuration

Since one of the primary considerations of this study has been reduction of the time required to obtain solutions, care has been exercised

to insure accuracy in the reported machine times. The machine configuration on which all work was performed is comprised of two coupled computers. The first, which performs such auxiliary functions as manipulating tapes, reading input cards, and printing output, is an IBM 7040. The second, which executes the problem submitted, is an IBM 7090. Separate records are kept of the times required by each in processing every problem. As only the time required to actually obtain a converged solution is of interest, the 7040 machine time was deleted from the reported solution times. All problems were also executed under the same operating system to avoid discrepancies in the calculation of auxiliary (i.e., exponential, trigonometric) subroutines. The reductions in solution time reported should, therefore, be quite accurate. Although the magnitude of the machine times may vary considerably on differing computer configurations, the time reduction ratio should be nearly constant.

Methods Developed

The pertinent features of the methods developed may be summed briefly:

(1) Multiple lower order or decoupled angular quadratures may be used to replace a higher order single quadrature set. One important feature of this option is that the number of characteristic directions may be increased without incurring negative point weights.

(2) Any progression of angular quadratures, in conjunction with arbitrary termination criteria, may be used to approach convergence. This method also allows the angular dependence of the flux to be made a function of the energy.

(3) The spatial mesh quadrature may be varied either by eliminating or combining mesh intervals. Direct use of this option, without further convergence, permits the calculation of problems having a variable spatial mesh.

(4) As a consequence of (2), it is possible to converge both the angular and/or scalar flux distribution to the same degree for any number of angular quadrature sets.

Conclusions

The first portion of this study was devoted to an attempt to eliminate or reduce the ray effect caused by the use of an insufficient number of characteristic directions in an S_n approximation. The procedure in (1) above has been shown to be partially effective. Its utility is limited by the fact that appreciable improvement is noted mainly in materials with a high scattering cross-section. While the ray effect may result in angular flux values which are either high or low, this procedure is most useful in correcting underestimates. Bounds may be applied to the method by noting that, in a pure absorber, solutions will be identical to those of the standard S_n method. In a pure scatterer, the method tends to approach the correct solution. However, since the ray effect is masked by scattering, so does the standard S_n technique. Thus, for materials with low scattering and high absorption cross-sections, only the use of a large number of characteristic directions can insure accuracy.

The second portion of this study developed several methods for allowing variations to be made in angular and spatial quadratures during

the course of an S_n calculation. Such methods have been shown to be quite successful in reducing the number of calculations required to attain a given degree of convergence in an S_n solution. For repetitive survey calculations, in which high accuracy is not required, the approximate solutions possible using the procedures in (2) and (3), (energy dependent angular quadratures and the combination or elimination of spatial mesh intervals) greatly reduce computation times and are more accurate than those yielded by merely solving a less detailed standard S_n case. While there may be some uncertainty regarding the quadrature order required to adequately describe a given energy group, the test case results have not varied greatly when reduced orders were used in groups expected to have nearly isotropic scattering. Moreover, the energy dependent quadrature solutions, particularly when combined with a low order preliminary quadrature, are a means for rapidly performing survey calculations. The combination or elimination of mesh intervals is more straightforward since the spatial configuration to be analyzed is known in advance. If the spatial mesh is reduced only in homogeneous regions removed from material interfaces, the approximate solutions are quite accurate.

For problem solutions in which accuracy identical to that yielded by the standard S_n method in a given spatial and angular approximation is required, the procedures in (2) and (3) above are capable of significantly reducing solution times. In addition, the test cases used allow some conclusions to be drawn regarding the optimum approach to convergence:

(a) Full convergence to the degree required of the final calculation should not be required for the preliminary quadrature sets.

(b) For problems having low order ($\leq S_8$) final angular quadratures, the most efficient approach to final convergence is through the use of a single preliminary S_2 quadrature followed by intermediate convergence on the final quadrature set.

(c) For problems having higher order ($>S_8$) final quadratures, the number of possible permutations in varying the angular quadratures is so large that specification of a general optimized procedure is impossible. The test cases show, however, that the solution time may be greatly reduced by the use of multiple preliminary quadrature sets.

(d) For problems using a less detailed spatial mesh to establish a preliminary scalar flux distribution, the optimum time to final convergence is observed when the preliminary mesh is relatively coarse.

One manifestation of ray effects in a calculation is that variation (change in order) of the angular quadrature set results in changes in the scalar flux distribution. Application of the procedure in (4) allows the fluxes in one order to be compared with the fluxes in a differing order. Appreciable discrepancies between the two approximations would be indicative of the presence of ray effects.

Summation

Use of the methods, and guidelines for their application, developed in this investigation have been shown to appreciably reduce the number of calculations and, consequently, the machine time, required to obtain solutions to the test cases used. The application of these methods to more

complex problems commonly being formulated may be expected to reflect even larger reductions in solution times. While analysis of the test cases has involved the use of only one type of quadrature variation at a time, there is no bar to combining the various methods for use in appropriate problems. The use of machine programs in which some of these combinations have been implemented indicate that time reductions of greater than fifty percent are not uncommon for larger, more detailed reactor configurations.

LIST OF REFERENCES

1. Boltzmann, L. Vorlesungen uber Gastheorie. Leipzig: Johann A. Barth, 1910.
2. Davison, B. Neutron Transport Theory. Oxford: The Clarendon Press, 1958.
3. Heading, J. Matrix Theory for Physicists. New York: John Wiley & Sons, 1963.
4. Wing, Milton G. Introduction to Transport Theory. New York: John Wiley & Sons, 1962.
5. Meghreblian, Robert V. and Holmes, David K. Reactor Analysis. New York: McGraw-Hill Book Company, 1960.
6. Lanning, W. D. "Application of the Spherical Harmonics Technique to Problems in Gamma Transport," Nuclear Science and Engineering, v. 15, No. 3, (1963), pp. 259-267.
7. Wick, G. C. "Uber ebene Diffusionsprobleme," Zeitsung fur Physik, v. 121, (1943), p. 702.
8. Chandrasekhar, S. Radiative Transfer. London: Oxford University Press, 1950.
9. Carlson, B. G. "Solution of the Transport Equation by S_n Approximations," Los Alamos Scientific Laboratory: LA 1891, 1955.

10. Carlson, B. G. and Lathrop, K. D. "Transport Theory - The Method of Discrete Ordinates," Los Alamos Scientific Laboratory, LA 3251 MS, 1965.

11. Lee, Clarence E. "The Discrete S_n Approximation to Transport Theory," Los Alamos Scientific Laboratory, LA 2595, 1962.

12. Carlson, B. G. "Development of the Discrete Ordinates Method," A Review of the Discrete Ordinates S_n Method for Radiation Transport Calculations. Edited by D. K. Trubey and B. F. Maskewitz, Oak Ridge National Laboratory, ORNL-RSIC 19, 1968.

13. Carlson, B. G. and Lathrop, K. D. "Discrete Ordinates Angular Quadrature of the Neutron Transport Equation," Los Alamos Scientific Laboratory, LA 3186, 1965.

14. Sangren, Ward C. Digital Computers and Nuclear Reactor Calculations. New York: John Wiley & Sons, 1960.

15. Carlson, B. G., Worlton, W. J., Guber, W., and Shapiro, M. "DTF User's Manual," United Nuclear Corporation, UNC Phys/Math 3321, 1964.

16. Barber, Clayton E. "A Fortran IV Two-Dimensional Discrete Angular Segmentation Transport Program," National Aeronautics and Space Administration, NASA TN D-3573, 1966.

17. Clark, M. Jr., and Hansen, K. F. Numerical Methods of Reactor Analysis. New York: Academic Press, 1964.

18. Cesari, L. "Sulla Risoluzioni dei Sistemi di Equazioni Lineari per Approssimazioni Successive," Atti accad. nazl. Lincei Rend., Classe sci. fis., mat e nat., v. 25, (1937), pp. 422-428.

19. Kopp, H. J. "Synthetic Method Solution of the Neutron Transport Equation," Ph.D. Thesis, University of Calcifornia at Berkeley, 1962.

20. Kopp, H. H. "Synthetic Method Solution of the Transport Equation," Nucl. Sci. Eng., v. 17, (1963), pp. 65-74.

21. Crawford, B.W. and Friedman, J. P. "Multigroup Two-Dimensional Neutron Transport," Trans. Amer. Nucl. Soc., v. 10, (1967), p. 172.

22. Gelbard, E. M. and Hageman, L. A. "The Synthetic Method as Applied to the S_n Equations," Nucl. Sci. Eng., v. 37, (1969), pp. 288-298.

23. Gelbard, E. M. "Outstanding Problems in Reactor Mathematics," Trans. Amer. Nucl. Soc., v. 8, (1965), p. 226.

24. Lathrop, K. D. "Ray Effects in Discrete Ordinates Calculations," Nucl. Sci. Eng., v. 32, (1968), pp. 357-369.

25. Kaplan, Stanley. "A New Derivation of Discrete Ordinates Approximations," Nucl. Sci. Eng., v. 34, (1968), pp. 76-82.

26. Brissenden, R. J. "The Parametric Point Method of Solving the Few Region Slab Transport Equation," Personal Communication, 1968.

27. Kaplan, Stanley. "Synthesis Methods in Reactor Analysis," Advances in Nuclear Science and Technology, v. 3, Edited by P. Greebler, New York: Academic Press, 1965.

28. Kaplan, S., Davis, J. A., and Natelson, M. "Angle-Space Synthesis-An Approach to Transport Approximations," Nucl. Sci. Eng., v. 28, (1967), pp. 364-375.

29. Natelson, M. "A Strategy for the Application of Space-Angle Synthesis to Practical Problems in Neutron Transport," Nucl. Sci. Eng., v. 31, (1968), pp. 325-336.

30. Sullivan, R. E., Yu, Dahsoong, Albers, Lynn U. "Reduction of Machine Time in Discrete Ordinates Calculations," Proc. Conf.: The Effective Use of Computers in the Nuclear Industry, CONF-690401, USAEC, 1969.

31. Joanou, G. D. and Dudek, J. S. "Gam II, A B_3 Code for the Calculation of Fast Neutron Spectra and Associated Multigroup Constants," General Dynamics Corporation, GA 4265, 1963.

32. Joanou, G. D., Smith, C. V., and Vieweg, H. A. "Gather II, An IBM 7090 FORTRAN II Program for the Computation of Thermal Neutron Spectra and Associated Multigroup Cross-Sections," General Dynamics Corporation, GA 4132, 1963.

33. Carlson, B. G., and Bell, G. I. "Solution of the Transport Equation by the S_n Method," Proc. of the Second UN Conf. on Peaceful Uses of Atomic Energy, v. 16, P/2386, Geneva: The United Nations, 1958.

34. Case, K. M., de Hoffmann, F., and Placzek, G. Introduction to the Theory of Neutron Diffusion, v. 1, Washington: US Government Printin Office, 1953.

35. Sullivan, R. E. "Comparison of S_n Codes," Memo. for Record, NASA Lewis Research Center, 1969.

36. Case, K. M., and Zweifel, P. F. "Existence and Uniqueness Theorems for the Neutron Transport Equation," J. Math. and Phys., v. 4, (1963), pp. 1376-1385.

37. Jorgens, K. "An Asymptotic Expansion in the Theory of Neutron Transport," Comm. Pure Appl. Math., v. 11, (1958), pp. 219-242.

38. Douglis, Avron. "The Solutions of Multidimensional Generalized Transport Equations and their Calculation by Difference Methods," Numerical Solution of Partial Differential Equations, Edited by James H. Bramble. New York: Academic Press, 1966.

39. Engle, W. W. and Mynatt, F. R. "One Dimensional Time Dependent Discrete Ordinates," Trans. Amer. Nucl. Soc., v. 12, (1969), p. 400.

40. Lathrop, K. D. "DTF-IV, A FORTRAN IV Program for Solving the Multigroup Transport Equation with Anisotropic Scattering," Los Alamos Scientific Laboratory, LA 3373, 1965.

41. Crawford, B. W. "An Iterative Solution Method for the Neutron Transport Equation with Anisotropic Scattering," Ph.D. Thesis, University of California at Berkely, 1965.

42. Mynatt, F. R. "Development of Two Dimensional Discrete Ordinates Transport Theory for Radiation Shielding," Ph.D. Thesis, University of Tennessee, 1969.

APPENDIX

NOMENCLATURE

g	index denoting the energy group
i,j,k	index denoting the rectangular mesh cell boundary in the x,y, and z directions
$\bar{m}$	residual vector equal to the difference between the exact and approximate result
n	neutron density
$\bar{r}$	generalized position coordinates
s	index denoting an interval in time
t	time variable
v	neutron velocity
w	weighting factor associated with a given angular direction
x,y,z	rectangular coordinate directions
A,B,C	rectangular mesh cell face area in the y-z, x-z, and x-y planes
E	energy variable
$\bar{F}$	Laplace transform of the function, F
G	total number of energy groups
I,J,K	total number of mesh cell intervals in the x, y, and z directions

$\overline{K}$ a vector which is constant during the course of a particular calculation

Q an extraneous neutron source

R reaction rate for a nuclear process

S total neutron source in a specified problem

$|a|$ the matrix, with elements a_{ij}, governing the angular flux calculation

$|\mathcal{O}|$ diagonal matrix

$|\mathcal{I}|$ identity matrix

$|\mathcal{L}|$ a lower triangular matrix, so defined that the diagonal elements are zero

$|\mathcal{M}|$ matrix used to denote an exact formulation of a problem

$|\mathcal{N}|$ matrix used to denote an approximation to the matrix, $|\mathcal{M}|$

$|\mathcal{S}|$ matrix, with elements s_{ij}, governing the scalar flux calculation

$|\mathcal{U}|$ upper triangular matrix, so defined that the diagonal terms are zero

δ Dirac delta function

η direction cosine with respect to the y axis

λ principal, or largest, eigenvalue, so defined that $(1/\lambda)$ is the effective multiplication factor

μ direction cosine with respect to the x axis

ξ direction cosine with respect to the z axis

σ macroscopic cross-section

ϕ scalar flux

ψ angular flux

$\underline{\psi}$ central average angular flux

$\hat{\Omega}$ unit direction variable